Università
Ca'Foscari
Venezia

Master's Degree programme (Second Cycle D.M. 270/2004) in
Conservation Science and Technology for Cultural Heritage

Final Thesis

Naples yellow and Pb-Sn-Sb yellow: characterization and evaluation of their stability through a multi-analytical approach

Supervisors

Prof. ssa Ligia Maria Moretto
Prof. ssa Karolien De Wael

Graduand

Laura Rabbachin
838746

A.A 2016/2017

CONTENTS

1. Introduction

1.1 History of the pigments

1.1.1 Lead antimonate yellow

Lead antimonate yellow, or Naples Yellow, is one of the most common yellow pigments used in Western European art, mainly in the period from 1500 to 1850[1]. However its history is much older and goes back to the early 2nd millennium BC. Along with Egyptian blue, lead antimonate is one of the oldest synthetically produced pigments known. It has been frequently identified as an opacifying and colorant agent in Egyptian glass from the 18th Dynasty (1550-1295 BC), period that coincide with the development of glass itself[2]. The pigment was also known in the Mesopotamian, Babylonian and Assyrian cultures where it was used as a colorant in glazed bricks and tiles[3]. Around the first and second centuries BC is reported that Naples Yellow was used by the Romans for yellow glasses[4].

As a pigment, lead antimonate yellow has been lost and rediscovered a number of times throughout history. After enjoying a great popularity in ancient cultures where it was the only yellow colorant and opacifier used in glass and glazes, it appears that in various parts of Europe, by the end of the 4th century A.D., the pigment was completely replaced by lead-tin oxide. Literature reports that during the Middle Ages lead antimonate yellow seems to have been limited to the Slavonian, Islamic[5] and Byzantine world as observed by Kirmizi *et al*. in late Byzantine glazed pottery from Turkey and the Former Yugoslav Republic of Macedonia[6].

Curiously 1200 years later (*c.*1500) the pigment reappears in the Western culture to be then again replaced within a relatively short period of time[3]. It's also not clear how Naples yellow re-emerged during the 15th century in Italian art. The most likely hypothesis is that the know-how on the production of lead antimonate was introduced by foreign artists, mostly Arab, to the Venetian glass workshops. Indeed, during the 15th century, after the fall of two main glass production centers such as Damascus (around 1400) and Constantinople (1452), two large waves of immigration of glassworkers from the Eastern Mediterranean to Venice are documented (1400

Syrian glass artists, 1453 glass artists from Byzantium)[1,5].

During the 16th century the production of Naples yellow is still closely connected with the glass and ceramic industries, as reported in many treatises from the time in which we can find the earliest recorded recipes. In 1540, Biringuccio, in his treatise *Pirotechnia* wrote about the use of antimony in making yellow glass enamels, while in the late 1550s, Piccolpasso published a treatise on the potter's craft (*Li tre libri dell'arte del vasaio*) that contains a series of recipes for lead antimonate to obtain yellow glazes on majolica. Another relevant reference about the production of Naples yellow in the glass industry is the Venetian *Darduin* manuscript (*Secreti per far lo smalto et vetri colorati*, 1644) where a collection of technical recipes on glass coloring can be found[1].

The first reference to Naples yellow as a **painting pigment** dates back to the early 17th century, when Valerio Mariani da Pesaro (1568–1625?) in his treatise about miniature painting, gives a detailed description of the production of so-called *giallo de' vasari* (potter's yellow), indeed the lead antimonate yellow. Mariani described three types of potter's yellow, including a recipe that considered the use of tin or zinc oxide. Before this time Naples yellow was already but sporadically used by some famous Italian artists like Lorenzo Lotto (1480-1556/7), Raphael (1483-1520), and Titian (1490-1576), that however still prefer the use of lead-tin yellow in most of their paintings[7]. Fig.1 shows a painting by Titian in which lead antimonate was probably used.

Fig.1 – *Girl with a basket of fruit*, Titian, 1555, Gemäldegalerie, Berlin, inv. 166

It's not always easy to confirm the use of this pigment on paintings considering that from the 14th century onwards various lead-based yellow pigments, notably the two types of lead stannate, the lead antimonate and the lead tin antimony oxide, all go under the name giallolino, which had caused, together with the similar composition, some misleading interpretation regarding the identification of the pigment.

From the second quarter of the 17th century Naples yellow begun to replace the traditional lead tin yellow pigment which falls in complete disuse by 1740[5,3]. By the beginning of 18th century Naples yellow becomes one of the most popular yellow pigments in European artists' palette. Canaletto (1697-1768), William Hogarth (1697-1764) and Joshua Reynolds (1723-1792) are just a few examples of painters that largely used it.

Naples yellow was much appreciated by artists for its intense bright hue, notably for giving a straw-colored both on yellow monochromatic areas and details. Due to its bright hue, it was also used for highlights and often mixed with green earths to obtain specific tints. As an example, Hogart mixes lead antimonate with blue pigments to achieve peculiar shades of green otherwise not obtainable with traditional green pigments.

Canaletto in his *San Rocco's celebration* (Fig.2) employs Naples yellow for the brownish-yellow color of the dresses, for the highlights and details on the architecture, and as a brushstrokes of pure color for light effects[7].

Fig.2 – *San Rocco's celebration*, Canaletto, 1735, National Gallery of Art, London

During the 18th century, when lead antimonate was introduced to Northern European painting, there was a widespread rumor according to which the pigment was a natural volcanic mineral found around the Mount Vesuvius in the Bay of Naples, hence the name Naples yellow was coined. The first reference to the name Naples yellow is the misleading Latin name *Luteolum Neapolitanum* given to the pigment by Andrea Pozzo in his treatise published in Rome between 1690-1700. Northern artists were not aware of the synthetic origin of lead antimonate since the handwritten recipes of Italian origin were intended for personal use and often kept secret by artisans. The production process of Naples yellow was not published until 1758 by the Italian Passeri, but the publication remained largely unnoticed in Northern Europe where the spread of knowledge about the real origin of the pigment has to be attributed to Fougeroux de Bondaroy (1769). Before then, lead antimonate was imported from across the Alps and only after the middle of the 18th century the production of this pigment started also in Northern Europe[5].

After enjoying its highest popularity in European art, from 1850 onwards it appears that Naples yellow was gradually replaced by cheaper and safer yellow pigments like lead chromate and cadmium sulfide.

Naples yellow was mainly used in oil on canvas, miniatures and only rarely on murals paintings[7]. In general it seems that the pigment was not recommended for watercolor painting (with an exception in Northern Europe during the 17th century) and in the *fresco* technique.

1.1.2 Lead-tin-antimony yellow

As mentioned previously, the identification and differentiation of lead-based yellow pigments on works of art has been difficult due to the confusing historical terminology of the pigments themselves and their reagents, vague information regarding their manufacture in ancient recipes, together with a lack of suitable scientific analysis for their characterization. This is especially the case of lead-tin-antimony yellow that was rediscover in the last decade of the 20th century, and only since then it has been unequivocally identified in artworks and distinguished from Naples yellow. Precisely, in 1998 Roy and Berrie announced the rediscovery of this pigment, based on its elemental characterization and identification on several seventeenth-century Italian paintings[8].

The history of lead-tin-antimony yellow is closely linked to the one of Naples yellow and like the latter, also finds its origin in the manufacturing of glass, enamels and majolica as an opacifying and coloring agent. According to Sandalinas and Ruiz-Moreno (2004)[9] the earliest recipes for the manufacture of a yellow pigment containing lead, tin and antimony appeared in the Venetian Darduin *Ricettario*, *Secreti per far lo smalto et vetri colorati*, a glass-manufacturing codex dating from 1644. Roy and Berrie suggest that the pigment originated as a by-product of the ceramic and glass industry and it was later adopted by painters in their palette.

The use of lead-tin-antimony yellow as a painting pigment spread throughout the 17th century in Italy. Roy and Berrie relate it specifically to paintings produced in Rome. In their work they identify the pigment in several artworks (from the 17th century) from different artists (O.Gentileschi, G.Lanfranco, Pietro da Cortona, N. Poussin and S. Rosa) all connected to the city of Rome.

It seems that this pigment was much appreciated by artists for its noticeably warmer hue (with orange tones) compared to other lead-based yellows. These color qualities made it perfect to achieve specific effects, particularly in the creation of golden-colored draperies. An example is given in *The Lute Player* by Orazio Gentileschi (Fig.3), where the dress of the young woman is painted with almost pure lead-tin-antimony pigment and is described as a "beautiful warm yellow"[8].

Fig.3 – *The Lute Player*, O. Gentileshi, *c.* 1612-20, National Gallery of art, Washington

However, the relation between lead-tin-antimony yellow and other yellows it's not clear and it's uncertain what caused simultaneous usage of Naples and Pb-Sb-Sn yellows. It is possible that the composition of these yellow pigments depended on the accessibility of the raw materials so their use was both temporally and geographically very specific[10]. Sandalinas and Ruiz-Moreno in 2004[9] confirmed the use of lead-tin-antimony yellow by many Italian artists from the 17th century and they identified the pigment in paintings by G.B Langetti and L.Giordano, both working in Venice in the 17th century. They also reported that the Spanish painter Velazquez used this pigment (most likely during his staying in Rome). In 2007 Hradil *and al.* studied the occurrence of Pb-Sn-Sb yellow in five Mid-European oil paintings from the 18th and 19th centuries[10] while recent studies[7] show that Pb-Sn-Sb yellow was used also by the famous English painter Joshua Reynolds.

Lead-tin-antimony yellow was not only used in oil on canvas but also on murals with *fresco* technique and on paper supports. It's found very often mixed with other pigments like ferric ochres (in warm yellows) and with Ultramarine and Prussian blue or green earths and copper greens to create different shades of green.[7,9,10]

1.2 Chemical composition and crystalline structure

1.2.1 Chemical composition

Lead antimonate $\mathbf{Pb_2Sb_2O_7}$ and lead-tin-antimony yellow $\mathbf{Pb_2SbSnO_{6.5}}$ are synthetic pigments produced by calcinating a ground mixture of antimony, lead and tin compounds, sometimes mixed with other materials. There is not one precise recipe to produce the pigments since many different ingredients were used during time, but it's possible to summarize the most common ones.

Lead compounds:

- metallic lead [Pb], lead monoxide [PbO], lead white [$2PbCO_3 \cdot Pb(OH)_2$], minium [Pb_3O_4], lead nitrate [$Pb(NO_3)_2$]

Antimony compounds:

- metallic antimony [Sb], antimony oxide [Sb_2O_3], potassium antimony oxide [$KSbO_3$], emetic tartar [$K(SbO)C_4H_4O_6 \cdot \frac{1}{2}H_2O$], antimony trisulfide [$Sb_2S_3$]

Tin compound:

- tin dioxide [SnO_2]

Other compounds (mostly used as flux agents):

- sodium chloride [NaCl], potassium hydrogen tartrate [$C_4H_4K_2O_6$], potassium carbonate [K_2CO_3], potassium nitrate [KNO_3], ammonium chloride [NH_4Cl], silicium oxide [SiO_2], sodium carbonate [Na_2CO_3], zinc oxide [ZnO]

The exact ratio between the elements, reaction time and temperature (between 700 and 1000 °C) are usually unknown parameters in the historical recipes and they vary significantly depending on the production methods, leading to different final products in composition and colour.

It is discussed in literature how artists chose their painting materials; if they choice of a Naples yellow instead of lead-tin-antimony yellow was only because of the specific hue or there was a knowledge of the production methods, hence of the chemical composition. It is possible that the composition of the pigments used by artists depended on the accessibility of the raw materials as well as on the cost. However, it does not have to be excluded that lead-tin-antimony yellow had some technological peculiarity[10], for which it was chosen compared to other yellow pigments.

1.2.2 Crystalline structure

Is known from literature[1-11] that both Naples yellow and lead-tin-antimony yellow belong to the class of cubic pyrochlore oxides. In particular lead antimonate yellow is the isostructural anhydrous analogue of the mineral bindheimite $Pb_2Sb_2O_6O'$, that however seems to be never used as a painting pigment[3].

The general formula for cubic pyrochlore oxides is $A_2B_2O_6O'$. A and B are metals and depending on their oxidation state, oxide pyrochlores can be classified as $A_2^{3+}B_2^{4+}O_7$ and $A_2^{2+}B_2^{5+}O_7$ types[12] (Naples yellow belongs to the second type $Pb_2Sb_2O_7$). The stability of this structure strongly depends on the ionic radius ratio (r_A/r_B)[13] with the A cation that must be appreciably larger than the B cation.

The pyrochlore structure, shown in Fig.4, can be described as two interpenetrating networks (B_2O_6 and A_2O'). The B cations (black spheres),

corresponding to Sb for Naples yellow, is six coordinated and located within an octahedra with oxygen atoms at the vertices; the BO_6 octahedra share all vertices forming large cavities. The A_2O' network consists, instead, of O' anions tetrahedrally coordinated with A cations (white spheres), corresponding to Pb for Naples yellow.

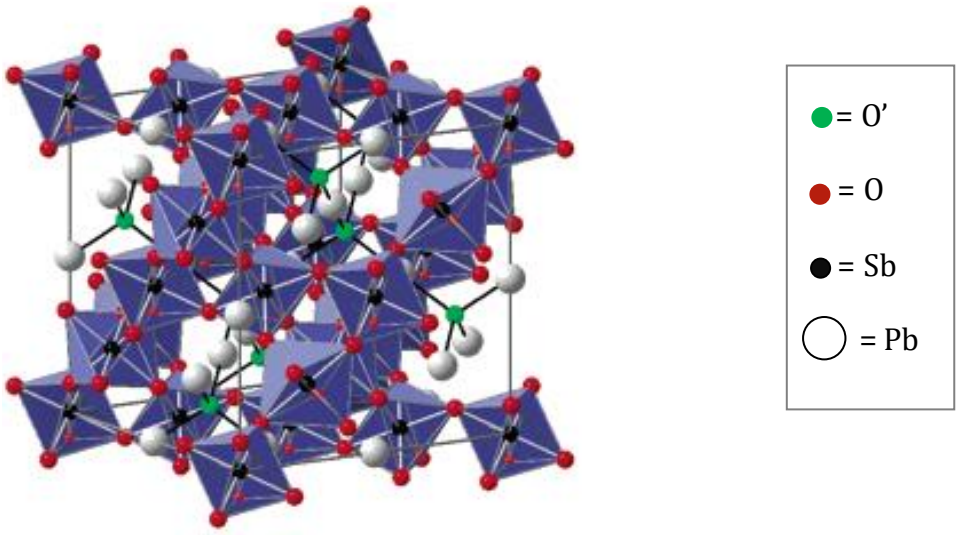

Fig.4 – Ideal crystal structure of pyrochlore compounds[14]

The two structures are interwoven such that the O' anions of the A_2O' network occupy the centers of the cavities formed between the BO_6 octahedra while A cations are positioned in hexagonal crowns formed by oxygen in the B_2O_6 framework. The O' ions are coordinate only with A cations, that have a final coordination number of eight, while the O ions are coordinate to two A and two B cations[11,12].

Pyrochlores are very interesting compounds because of the possibility of a wide variety of chemical substitution at the A and B sites. The structure also tolerates vacancies at the A and O sites allowing cation migration within the solid. These compounds exhibit also an exceptional range of physical properties that goes from a highly insulating through semiconducting to metallic behavior that can be controlled by doping[13,15].

In the pyrochlore structure of lead-tin-antimony yellow the third cation Sn^{4+} enters in the lead antimony phase replacing some of the Sb^{5+} ions in the octahedral (SbO_6) sites [1,10,11,16]. Cartechini *et al.*[16] and Hradil *et al.*[10]report that the introduction of tin (larger than antimony) in the binary pyroantimonate leads to an expansion of the lattice size and to a distortion of the local symmetry of the Sb-O polyhedra.

It has been reported in literature that it is difficult to synthesize Naples yellow and lead-tin antimony yellow with pure pyrochlore structure. Usually, in the pigments, by-products can be observed. As seen before, to facilitate the production of a homogeneous powder and also to improve the colour, historical recipes suggest, during the calcination process, the use of flux agents, which are a common way to enhance the crystal growth[10]. However, the addition of these compounds might leave a residue in the final product. NaCl and related compounds like oxychlorides are found only after short calcination times and with the temperature kept below 800 °C [3,10]. Nonetheless chlorine can react with the other reagents forming products containing Pb and Cl as pointed out by Agresti[7] who suggested that Cl can be present in the lead antimonate lattice (Cl-Pb-Cl bond). Hradil *et al.* reported that, with an excess of wine lees (K_2CO_3), K is either converted to potassium antimonate or remained unconsumed. In some cases K might also be present in the pyrochlore lattice[10]. Also Dik *et al.* found that in the Naples yellow calcinated with K-tartrate, by-products containing potassium can be detected, e.g. $K_2NaSb_3O_9$ and $K_3Sb_3O_9$. Moreover, Naples yellow can present more than one phase of $Pb_2Sb_2O_7$ with slightly different unit cells, which seems to depend on the ratio of Pb and Sb.

With respect to lead-tin-antimony yellow, small amounts of SnO_2 are always found in the final compound[1,9,10] because of incomplete reaction of the starting materials. It seems that calcination temperature (680-1000°C) together with the proportions between the base oxides (PbO, SnO_2 and Sb_2O_3) are very important parameters to determine the composition of the pigment obtained. To produce a final compound containing for the most part pyrochlore $Pb_2SnSbO_{6.5}$ and only a negligible quantity of SnO_2, the molar ratios of the reagents needs to be Pb:Sn:Sb = 2:1:1. A variation in the stoechiometry of the base oxides will lead to a heterogeneous pigment powder mixed with other compounds.

1.3 Degradation of the pigments

A pigment is define as an insoluble coloring substance which, mixed with an aqueous or oily media, is able to impart color to objects through a covering layer. Pigments are mainly inorganic materials, with the exception of lake pigments (organic); they can be natural, if coming from minerals and earths, or synthetic, if man-made by chemical processes.

Pigments have a wide variety of characteristics and properties but there is one thing almost all of them have in common: they degrade over time. Degradation occurs in very different ways involving chemical and physical processes, often combined together. Considering that color is probably the most important property in a art object, especially in paintings, many researchers focused their attention on pigment degradation. What it is perceive as a change in the color properties (fading, discoloration, darkening) corresponds most of the time to a specific chemical/physical process (a change in the crystalline structure, a reduction/oxidation process, formation of new compounds etc.). It is not always easy to study and understand degradation phenomena, most of the time because the number of parameters implicated it's huge (light, moisture, binding medium, interaction between incompatible pigments, influence of particulate matter...) and the effect is synergetic.

Studies on pigment degradation usually focus on chemical analysis of historical paint samples and monitoring studies of model samples aged under specific conditions[17]. In order to do so, XRD, SEM-EDX, FTIR and Raman spectroscopy are some of the classical techniques employed. More advanced methods based on X-rays synchrotron radiation have recently permitted a better insight in the alteration mechanism of some pigments such as vermillion, Prussian blue, smalt, cadmium yellow and lead chromate[18]. Recent studies[19,20,21,22] focused their attention on light-induced pigment degradation using also a new approach based on (photo)electrochemical methods. In particular some semiconductor pigments were investigated considering the potential synergistic effect of light exposure and particulate matter (PM). Indeed, in the last years, the impact of the air quality inside museum on complex objects of cultural relevance has raised interest and factors like

illumination conditions, inorganic pollutants, and volatile organic compounds have been studied[23].

1.3.1 Pb-based pigments degradation

In general lead-based pigments can be affected by sulfur containing pollutants, acid solutions (rain, CO_2, microbial activity) and light, leading to a wide variety of degradation products, such as $PbSO_4$, $PbCO_3$, $2PbCO_3{\cdot}Pb(OH)_2$ and PbS, that strongly affect the pigments appearance. Some lead-based pigments (lead-white, massicot, red lead) and their degradation products are sensitive to light and a reduction of the lead compounds occurs on the surface of artworks with the formation of metallic lead and/or PbO_2, or, in the case of red lead a darkening can be observed (lead(IV) oxide). All lead pigments are reported to turn black after exposure to H_2S vapors due to the formation of PbS[23].

Organic pollutants, such as acetic acid and formic acid, often present in museums, can also affect Pb-based pigments as pointed out in a recent study by De Laet *et al.* that shows how red lead, lead white and lead-tin yellow degraded towards lead acetate after exposure to acetic acid vapors[24].

Lead pigments are known to be good driers in oil paintings and they were sometimes added intentionally in mixture with other pigments as siccatives in order to guarantee a better polymerization of the oil. On the other hand lead pigments, when in contact with oil, are also known to form lead soaps (metal ions + fatty acids), which negatively affect the appearance of the paintings. Higgitt *et al*. report that the formation of lead soaps is related to the presence of available Pb(II) ions in the pigment mixed with the oil[25].

1.3.2 What is known about the degradation of $Pb_2Sb_2O_7$ and $Pb_2SbSnO_{6.5}$?

Little is known about the degradation of Naples yellow and no references were found about lead-tin-antimony yellow. Coccato *et al.* report that Naples yellow is known to degrade but they do not consider the pigment in the cited study[23]. In Analytical Chemistry for Cultural Heritage the degradation of Naples yellow is also mentioned, however is not later expalined[26]. In the section about lead antimonate yellow in *Artists' pigments*[3], Naples yellow is described as alkali-fast, insoluble in

organic solvents and because of the presence of lead darkened by atmospheric hydrogen sulfide. Concerning the pigment-medium interaction two specific cases about Naples yellow are found in literature : (1) Keune *et al.*[27] described the presence of lead soaps in naturally and artificially aged Naples yellow-containing linseed oil paint samples, while (2) Tumosa *et al.* [28] reported a study by Van der Weerd[29] showing, in presence of Naples yellow, the hydrolysis of the oil as well as lead soaps formation by means of FTIR.

There is an interesting issue about Naples yellow being affected by contact with iron, well summed up by Wainwright *et al*. in *Artists' pigments*[3]. The authors report that in 1764 Dossie voiced the belief that the use of a metal palette knife might cause the discoloration of lead antimonate. Field (1835) adds that not only metal palette knife are dangerous for Naples yellow but also warns about mixing this pigment with any iron-containing pigments such as ochre or Prussian blue[30]. Later authors (Stokier, Church, Doerner) remarked that lead antimonate yellow is affected by iron, but they also report that the mixture with iron-containing pigments does not have any effect. Specifically Church (1915) reports that:

> "*true Naples yellow is undoubtedly spoilt by contact with a steel spatula, because the metal of the latter takes away oxygen from, or ' reduces ' the lead antimonate of which the former consists. But such an action is impossible with yellow ochre, for this iron compound is a stable substance, containing already all the oxygen it can take up*" and again *"Naples yellow, in contact with metallic iron, tin, pewter, zinc, and several other metals, is discoloured and blackened. An ivory instead of a steel spatula, or palette knife, should be used with this pigment. The darkening in question is due in part to attrition, owing to the extreme hardness of the particles of the lead antimoniate, however finely the material may have been ground, and partly to the reducing effect of the above-named metals upon this antimoniate. Iron in the form of its oxide or hydrate (as in light red or yellow ochre), or in complex combinations (such as Prussian blue), does not exert any effect upon Naples yellow."* [31]

Wainwright *et al*. hypothesized that the changing to gray or grayish green is due to residual chlorides or other impurites reacting with iron and forming iron chloride or other compounds[3]. Interestingly, even nowadays, the producer of the lead antimonate used for this study (Chap.3 - 3.1 Samples) declares that Naples yellow "because it tends to react when parsed with steel rollers, to this day" he "still grind it with stone"[32].

According to Church[31] Naples yellow is darkened by Cadmium yellow and it is affected or it affects organic pigments such as Indian yellow and red lakes. Moreover lead antimonate yellow is reported to be unstable in contact with Barium yellow *in fresco*[3].

2. Aims of the thesis

The aim of this thesis is the evaluation of the stability under different aging conditions of Naples yellow ($Pb_2Sb_2O_7$ – LAY) and the less known lead-tin-antimony yellow ($Pb_2SbSnO_{6.5}$ - LTAY) pigments. In the last years a renewed interest on the production and identification of these pigments raised from the scientific community, but still little is known about their degradation.

The first goal was to gather a good knowledge of the elemental composition and crystalline structure of the pigments, necessary before proceeding with degradation studies. Therefore, in order to achieve a complete characterization of the pigments, X-ray fluorescence (XRF), μ-Raman spectroscopy (μ-RS) and X-ray diffraction (XRD) were employed. In addition colorimetric measurements were carried out to describe the hue of the pigments used in this work.

The ultimate aim of this thesis, was to study the behaviour of the two pigments under different aging conditions. The starting point was to evaluate the pigments sensitivity to light. Since recent studies pointed out that some inorganic yellow pigments, such as cadmium yellow and chrome yellow, act like semiconducting materials, hence sensitive to light, the aim was to study if Naples yellow and lead-tin-antimony yellow might also have the same properties. In order to do so a new approach based on DR-UV-Vis spectroscopy and photo-electrochemical methods was employed. In addition, experiments using lights at different wavelengths (green 514.5nm, blue 405 nm, UV ~300nm) were carried out. μ-RS and colorimetry were used to monitor the eventual light-induced degradation.

The second part of this thesis was aimed to investigate the chemical stability of the two yellow pigments. Two common organic pollutants (acetic acid and formic acid) in museum environments were chosen for an initial study, the aim is also to verify if under exposure to their vapors tin might have an influence in the eventual degradation process, as recently noticed in literature for Pb-Sb-Sn alloys.

After these tests, samples and eventual degradation products were characterized with μ-Raman spectroscopy, XRD and SEM-EDX. A possible color change was evaluated by colorimetric measurements.

3. Materials and methods

3.1 Samples

For this study, two pigment powders and one commercial oil paint were used. The Naples yellow and lead-tin-antimony yellow pigments were produced at the Department of cultural heritage sciences of the University of Tuscia (Viterbo, Italy), according to the following recipes.

Naples yellow, $Pb_2Sb_2O_7$, (**LAY**) was synthesized according to an ancient recipe by Piccolpasso in *Li tre libri dell'arte del vasaio* (*Zallolino A*):

- Lead(II,IV) oxide (minium), Pb_3O_4 = 4,91 g
- Antimony oxide, Sb_2O_3 = 3,27 g
- Potassium tartrate (wine residue), $C_4H_4K_2O_6$ = 2,76 g
- Sodium chloride, NaCl = 2,76 g

The reagents were mixed in a agate mortar and the obtained powder was put in the kiln on a terracotta tile for 5 hours at 800 °C.

Lead-tin-antimony yellow (**LTAY**) was synthesized according to the stoichiometric ratio of the chemical elements in the final compound ($Pb_2SnSbO_{6.5}$):

- Lead monoxide (litharge), PbO = 8,90 g
- Antimony oxide, Sb_2O_3 = 2,90 g
- Tin dioxide (cassiterite), SnO_2 = 3,00 g

The reagents were mixed in a agate mortar and the obtained powder was put in a kiln on a terracotta tile for 5 hours at 925 °C.

The commercial oil paint (**NG**) belongs to the series Michael Harding's artists oil colors[35] and it is named *Genuine Naples Yellow dark* (No.606). As reported in the website the paint is supposed to contain a "genuine pigment" mixed with a very low quantity of linseed oil. The pigment is indicated as PY 41, corresponding to lead antimonate in the Color Index (Fig.5).

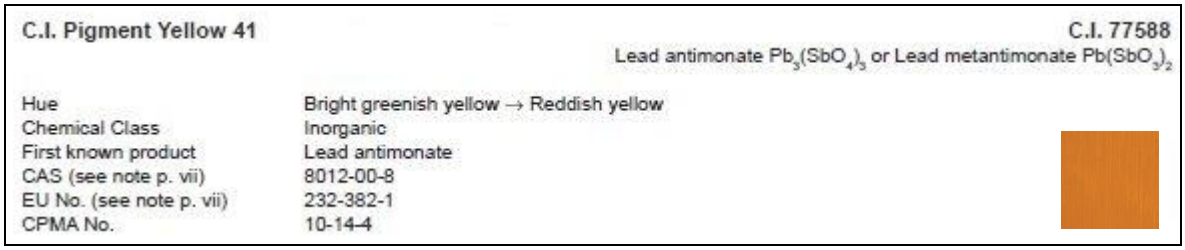

Fig.5 – Technical data of PY 41 in the Color Index

The color is described as a "warm, dense, almost ochre yellow [...] more powerful and yet more muted than its equivalents among the Cadmium range".

The reagents, calcination temperature and reaction time are not indicated. It is declared on the website that the colors produced by Michael Harding do not have any filler in order to extend the volume of the oil paint and neither contain any drier.

3.1.1 Mock-up paint samples preparation

Mock-up paint samples were prepared in order to do some degradation experiments and simulate a more realistic situation compared to the pure powders. Indeed, pigments are always mixed with a binding medium in paintings. In this way it is also possible to evaluate the influence of the binder in the degradation processes. For this work linseed oil was chosen since it is one of the most commons binders from 15th century onwards. Moreover it is known that in artworks Pb-based pigments can react with the drying oils to form metal soaps (see *1.3.1 Pb-based pigment degradation*).

Mock-up samples were prepared by grinding the pigment powders with the linseed oil on a container with a glass mortar and a knife palette (Fig.6 - a) until a workable paint was obtained.

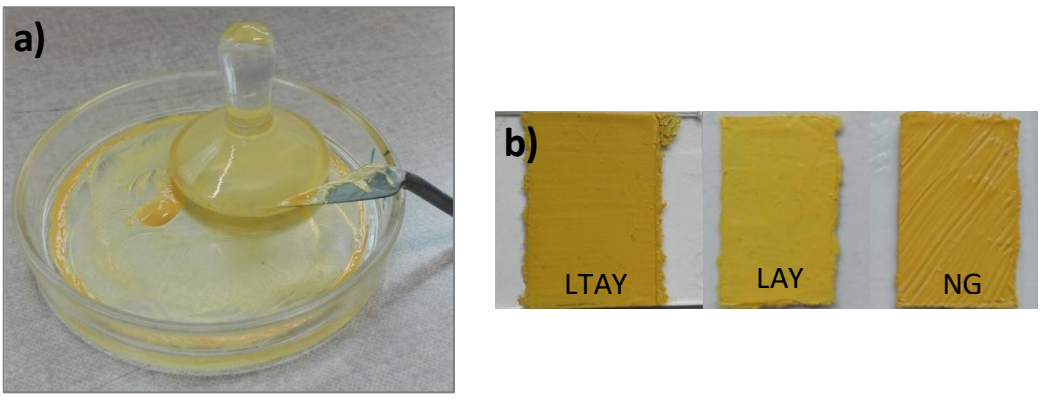

Fig.6 – Preparation of the oil paint (a) and the three paints applied on the plastic slide (b)

The obtained mixtures (LAY and LTAY paints), together with the commercial oil colour (NG) were applied with a spatula or a brush on polycarbonate microscopy slides (Fig.6 – b) and they were left to dry naturally. Mock-up samples measure approximately 2 x 2.5 cm.

The paints were spread as flat as possible in order to reach a homogeneous degradation. Irregular samples with *impasto*, although they recreate a more realistic situation, might degrade unevenly depending on the area of the sample. This situation entails too many parameters, which is not an ideal condition for a preliminary study.

3.2.2 Cross-sections preparation

In order to check if a degradation layer was formed after aging experiments thin cross-sections of the mock-up samples were prepared and analyzed with Raman spectroscopy and SEM-EDX. Cross-sections were prepared by cutting part of the mock-up samples of interest and embedding them in acrylic resin (ClaroCit Powder: dibenzoyl peroxide and polymerised methacrylic esters, mixed with ClaroCit Liquid: methyl methacrylate and tetramethylene dimethacrylate, Struers). After drying, cross-sections were first cut with a saw to remove the resin in excess and later a rotary microtome (HM360, MICROM International GmbH, Walldorf, Germany) was used to make the thin cross-sections (50 μm), which were fixed on plastic slides. Subsequently cross-sections were observed and photographed with an optical microscope Olympus BX 41 (Olympus America Inc., New York, USA) with incident light and magnification up to 50x.

3.2 Experimental procedures

3.2.1 Irradiation experiment with blue laser

For aging purposes, mock-up samples (LAY, LTAY and NG) were illuminated with a blue laser (405 nm) with maximum power of 50 mW. After the irradiation Raman measurements were carried out to check if changes in the Raman spectra were visible, hence the pigments had degraded. To make sure the Raman measurements were acquired on the same spot previously illuminated with the blue

laser a mask was applied on the samples, as illustrated in Fig.7. The mask was created with a plastic slide in which some holes were made with a diameter of approximately 2 mm (smaller than the beam size of the laser) and it was fixed on the mock-up samples with some tape.

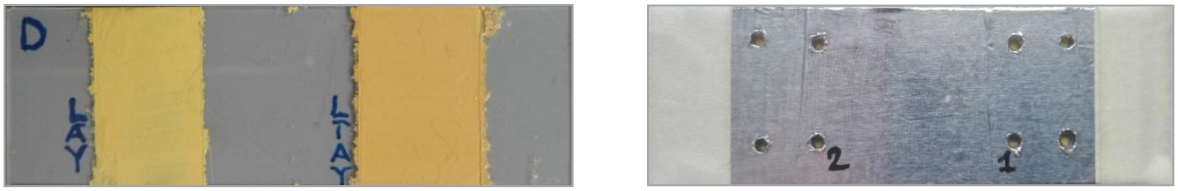

Fig.7 – Example of the mask covering the mock-up samples

As shown in figure 8 the samples with the mask were attached on a polystyrene cube at the laser's pointing area level. Everything was covered with a security black box. LAY and LTAY were illuminated for 1, 2 and 24h, while NG only for 2h.
The power of the laser beam was measured before and after the experiments with a laser power meter to verify it didn't change during the illumination.

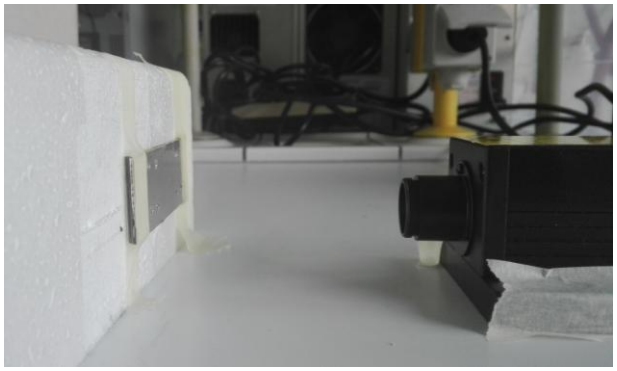

Fig.8 – Set-up for the blue laser experiment

3.2.2 Climate chamber (UV aging)

In order to speed up deterioration processes the climate chamber is a useful tool widely used in the cultural heritage field. Indeed it allows to age materials and predict their stability under controllable and reproducible conditions (light, temperature, humidity) in a laboratory environment and in a relative short time. Though, it is necessary to be careful when evaluating the stability of a material artificially aged, especially if more than one chemical process is involved in a particular alteration. It might happen that a change in the aging conditions will not speed up each process to the same extent[17].

The climate chamber used to age the mock-up paint samples of LAY, LTAY and NG had only a UV light (530 W/m^2) and a temperature of around 30°. No humidity was involved. The samples were aged for 1000h.

3.2.3 Chemical aging

In order to investigate the chemical stability of the pigments, preliminary experiments with acetic (CH_3COOH) and formic (HCOOH) acid were carried out. To expose the pigment powders and mock-up samples to the acids vapors, samples were placed in a dessicator that allowed to maintain a controlled environment.

For the first experiment, about 20 ml of concentrated (99%) glacial acetic acid (Sigma-Aldrich) were put in a becker that was positioned in the bottom of the dessicator. The pigment powders (LAY and LTAY), previously attached on adhesive tape and fixed on plastic slides, and the mock-up samples (LAY, LTAY and NG) were placed onto a support (experimental set-up is shown in Fig.9). Samples were exposed to the vapors for two weeks. After taking them out of the dessicator, since a wet layer was formed on the mock-up samples, they were left to dry and later analyzed.

The same procedure was followed for the formic acid (99%, Sigma-Aldrich). The two experiments were repeated only with the mock-up samples with an exposure time of four weeks.

Fig.9 – Experimental set-up for the exposure of the pigments to acetic and formic acid

3.3 Analytical techniques

3.3.1 Micro-Raman Spectroscopy (μ-RS)

Micro-Raman spectroscopy is a molecular analytical technique that relies on inelastic scattering, or Raman scattering, of monochromatic light. When monochromatic light, usually from a laser, interacts with the sample, molecules are excited into a "virtual" state, highly unstable, decaying instantaneously and emitting photons. Fig.10 illustrates an energy level diagram showing the excitation-relaxation phenomena responsible for the different scattering. Most of the photons are scattered elastically, whereby the emission of a photon of the same energy than the incident one allows the molecule to relax to its ground vibrational state (*Rayleigh scattering*). A small portion of light is, instead, scattered inelastically, involving transfer of energy from the photons to the molecules or vice versa. The scattered photons have different energy than the incident ones (*Raman effect*). There are two types of Raman scattering; when the molecule decays at an excited vibrational state emitting a photon with lower energy ($h\nu_0 - h\nu_1$) than the incident one ($h\nu_0$), the Stokes Raman scattering occurs (b), while the anti-Stokes Raman scattering is caused by a molecule that, already present in a excited vibrational state ($h\nu_1$), decays from the virtual state to the ground electronic state, emitting a photon with higher energy ($h\nu_0 + h\nu_1$) than the incident one (c). The energy shift gives information about the vibrational modes in the molecule, so a structural fingerprint is obtained and molecules can be identified.

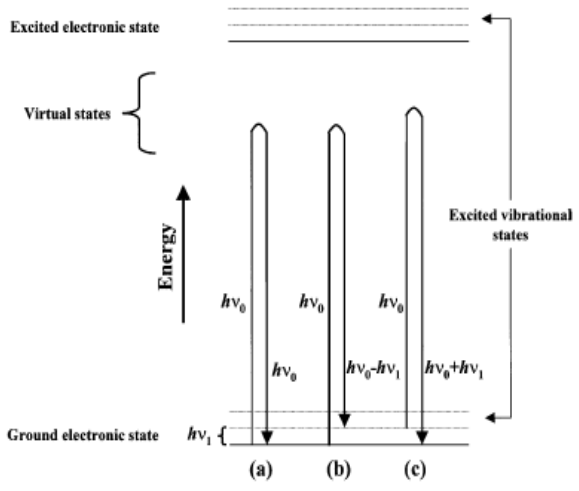

Fig.10 – Energy level diagram. Rayleigh(a), Stokes (b) and anti-Stokes (c) Raman scattering

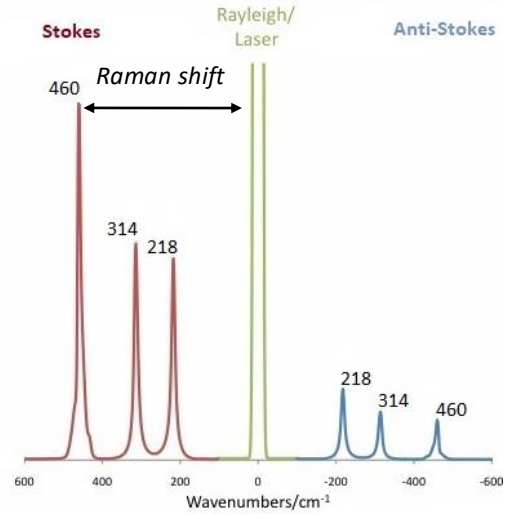

Fig.11 - Stokes /anti-Stokes Raman bands. (readapted from http://www.raman.de/)

In the Raman spectrum, an example is given in Fig.11, intensity of scattered light (y-axis) is plotted against the absolute frequency of light (x-axis) or, most commonly, against the *Raman shift,* that is the difference in wavenumbers (cm^{-1}) between the observed radiation and the incident one. Stokes and anti-Stokes lines are symmetrical compared to the Rayleigh line. Normally the part of the spectrum with Stokes bands is the one used for diagnostic purposes since the intensity of the signal is higher than the anti-Stokes signal.

Raman spectroscopy gives information about molecular and crystal lattice vibrations, therefore is sensitive to the composition, bonding, chemical environment, phase, and crystalline structure of the sample material. The analysis can be performed on materials in any physical form: gases, liquids, solutions, and crystalline or amorphous solids[36].

Its non-destructiveness, speed, high spatial (≤ 1 μm) and spectral resolution (< 1 cm^{-1}), relative immunity to interference, applicability to unprepared samples of large or non-uniform shape as well as inhomogeneous samples and with a complex matrix, make Raman spectroscopy well suited to the study of historical and art materials[37]. In particular Raman spectroscopy can be applied for pigment identification and to probe their degradation and stability.

In this thesis μ-RS was used:

- to verify the crystal structures of the pigments and to characterize them;
- to analyze the samples after different aging conditions and detect possible degradation products;
- to induce degradation with the green laser (514.5 nm) and simultaneously acquire the spectra in order to investigate the pigments' sensitivity to light;

μ-RS spectra were acquired with a Renishaw inVia multiple laser Raman spectrometer with a Peltier-cooled (203K), near-infrared enhanced, deep-depletion CCD detector (576x384 pixels) and coupled to a Leica optical microscope. The instrument was calibrated using a silicon wafer. Raman spectra were collected using both a continuous wave diode laser operating at 785 nm wavelength (red) in combination with a 1200 l/mm grating with a maximum laser output power of 300mW and a air cooled argon laser (Stellar-Pro 514/50) operating at 514.5 nm

wavelength (green) in combination with a 1800 l/mm grating with a maximum laser output power of 50mW. The laser was focused onto the samples through 50x objective achieving a spatial resolution of a few micrometers. Depending on the sample analyzed, the laser (red or green) and the power were changed. Precise parameters are given when discussing the spectra. Exposure time varied between 10 and 60 seconds with 1 up to 10 accumulations to obtain an adequate signal-to-noise ratio. Measurements were repeated from 5 up to 10 times for each sample. Data acquisition was carried out with Renishaw WiRE 2.0 software.

3.3.2 Diffuse Reflectance UV-Vis Spectroscopy (DR-UV-Vis)

Diffuse reflectance UV-Vis spectroscopy is one of the most employed optical methods to calculate the band gap. In the absorption spectrum, at a given wavelength, there is an increase in the absorbance that indicates the optical excitation of the electrons from the valence band to the conduction band[38]. The linear section in the diffuse reflectance spectra is taken for measuring the band gap energy; by extrapolating the linear portion of the absorption curve with the wavelength axis, the absorption wavelength is deduced and converted to the band gap energy[19,21]. To calculate the band gap energy (E_g) the following equation is used:

$$E_\gamma = h\nu = \frac{hc}{\lambda}$$

where (h) is the Planck's constant = 6.626 x 10^{-34} J·s = 4,136 x 10^{-15} eV·s and (c) the velocity of light = 3 x 10^8 m/s. The equation can be re-written as:

$$E_g = \frac{1240}{\lambda}(\text{eV})$$

DR-UV-Vis spectroscopy was used to obtain absorption spectra in order to determine the band gap energy of the pigment powders.

DR-UV-Vis measurements of Naples yellow and lead-tin-antimony yellow were carried out with an Evolution 500 UV-Vis double-beam spectrophotometer with RSA-UC-40 DR-UV integrated sphere, Thermo Electron Corporation, Waltham, Massachusetts. The pigment powders were mixed and crushed with KBr dried at 200°C (0.02 g of pigment powders in 0.98 g KBr). The mixtures were homogeneous

and positioned in the DR-UV-Vis cell for measuring in the 250 to 800 nm range. The measurements were carried out in collaboration with the LADCA research group (University of Antwerp, Department of Chemistry).

3.3.3 Photo-electrochemistry

The aim of this experiment was to check if the pigments (LAY and LTAY), develop a photo-current under irradiation of a laser, hence they were reactive to light . In order to do so, potentiometry (OCP) and amperometry (with the use of a laser) were employed.

Potentiometry is a non-dynamic electrochemical method in which the potential is monitored in function of time. Amperometry is instead a dynamic electro chemical method that measures the current in function of time at a imposed potential. Details on the measurements are given below.

Electrochemical set-up

Graphite rods working electrodes were prepared by mechanical polishing with a P800 SiC paper. The electrodes were rinsed with deionised water and ethanol in an ultrasonic bath for 15 s each to remove any adherent SiC particle. In order to deposit the pigments on the working electrode, suspensions of 50 mg of LAY or LTAY pigment powder in 1 mL of ethanol were prepared. With a micropipette a drop of 1.5 µL of the suspension was deposited on the working electrode and left to dry. A thin layer of the respective pigment was formed after solvent evaporation. The modified electrodes are denoted as G|$Pb_2Sb_2O_7$ and G|$Pb_2SbSnO_{6.5}$, referring to the electrode material followed by the respective pigment. As illustrated in Fig.12 the working electrode (W.E.) was mounted in an open container with the pigment-modified side oriented upwards, so that pigment irradiation with a 30 mW blue laser (405 nm) pointing downward was possible. The container was subsequently filled with 6mL of electrolyte solution (1 mM NaCl). A silver-silver chloride (Ag|AgCl) in saturated KCl electrode was used as reference electrode (R.E.) and was protected from light illumination by covering it with aluminum foil. To complete the electrochemical cell a glassy carbon rod (GC) or platinum electrode (Pt) were used as counter electrodes (C.E).

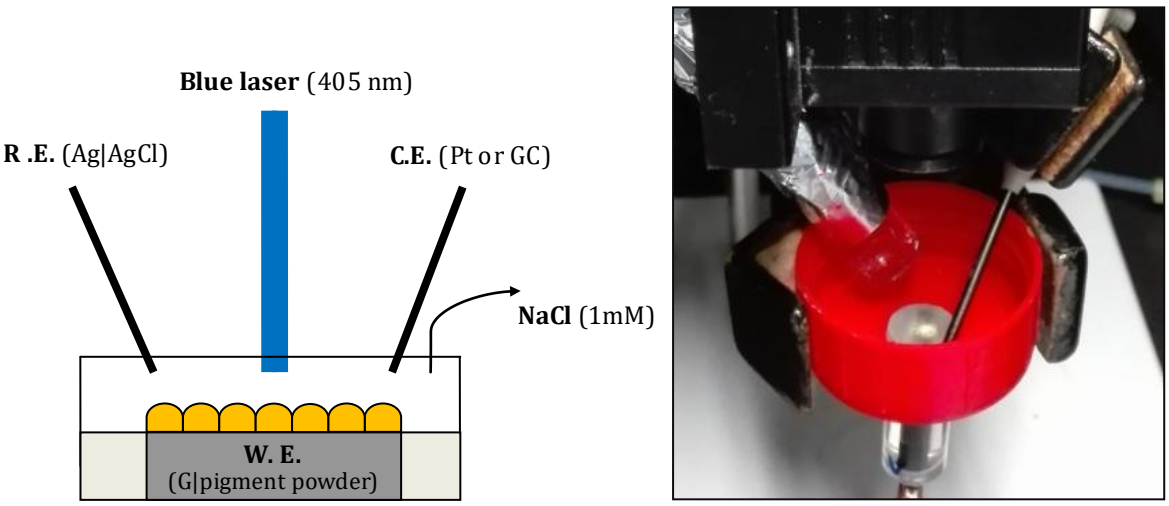

Fig.12 - Scheme of the cell with the relative parameters and picture of the electrochemical set-up with the pigment-modified working electrode oriented upwards

Open circuit potential (OCP) and amperometry

The open circuit potential is the potential of the working electrode (in this case the pigment-modified working electrode) relative to the reference electrode when no potential or current is being applied to the system. Generally, the OCP of an electrode is a thermodynamic parameter that gives information about the thermodynamic tendency of the material to participate in the electrochemical reaction with the surrounding medium. A potential below OCP is more thermodynamically stable, while a potential above OCP is thermodynamically unstable, so more prone to react.

After ~250 s of measurement of OCP the blue laser was switched on for 10 s. After other 250 the OCP was considered stable. The instrument automatically calculates an average value of the last 100 s of the OCP measurement and it applies that value in the amperometric experiment, in order to avoid a possible degradation process by applying a non-equilibrium potential. In this way it is possible to reach a situation comparable to a "natural" environment.

During the amperometric measurement, the photo-current of LAY and LTAY was monitored over time. Five alternating cycles of darkness (~10 s) and illumination (~30 s) with a blue laser (405 nm) were applied.

All the electrochemical experiments were performed with an Autolab PGSTAT101 potentiostat (Metrohm, The Netherlands) controlled by NOVA 1.10

software.

No photo-electrochemical experiments were performed on the commercial Naples Yellow (NG) since the binding medium contained in it would have probably interfered in the measurements.

3.3.4 X-Ray Fluorescence (XRF)

XRF analysis is an non-destructive technique of semi-quantitative elemental analysis based on the detection of the X-ray fluorescence emitted by a sample being irradiated by an energetic beam of primary X-rays. The energy of the fluorescent photons is the difference in energy between the vacancy, that is the result of the ionization process, and the electronic state of the electron filling the vacancy[29]. The characteristic radiation emitted by the ionized atoms contains information on the nature and the abundance of the elements in the sample; specifically in the XRF spectrum the energy is connected to the nature of the elements present in the sample, while the intensity (counts) is connected to their abundance[39].

XRF was used to verify the elemental composition of the pigments, especially for the NG sample since, being a commercial paint, the composition was uncertain.

XRF spectra were acquired with a Minipal-2 (Panalytical) spectrometer , which is equipped with a low power, air-cooled Rh-anode X-ray tube and a Si-PIN detector. The Minipal-2 has a maximum power, current and voltage of respectively 9W, 1000 μA and 30 kV. All samples were measured with a live time of 1000 s by applying a voltage of 30 kV and current of 3 μA and using a 50 μm Al filter between the X-ray tube and the sample. All spectra were analysed using the bAXIL software package (BrightSpec).

3.3.5 Colorimetry

Colorimetry quantitatively measures the reflection properties of a material as a function of wavelength, describing in a objective and mathematical way the human colour perception. A colorimeter can detect minimal colour changes, not perceptible at the human eye. Colors can be represented in the CIEL*a*b* colour space, illustrated in Fig.13, where the total colour change, ΔE, is calculated as the distance between two points, using the following formula:

$$\Delta E = \sqrt{(\Delta L^{*2} + \Delta a^{*2} + \Delta b^{*2})}$$

where L* represents the lightness of the colour with values going from 0 (black) to 100 (white), a*expresses the colour red when positive and the colour green when negative while b* expresses the colour yellow when positive and the colour blue when negative. a* and b* axes have values going from +infinite to -infinite.

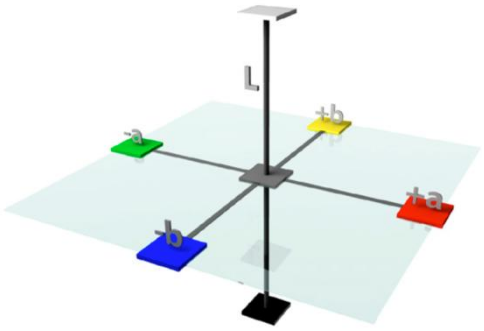

Fig.13 – CIEL*a*b* color space[40]

Colorimetry was used to describe the hue LAY, LTAY and NG and evaluate the colour changes of the mock-up samples before and after degradation experiments .

The colorimetric measurements were performed with an AvaSpec-2048 L, coupled to an AvaLight-DH-S-BAL light source and controlled with AvaSoft 7.5 (Avantes BV, Apeldoorn, The Netherlands). The optical system has an integrating sphere with a angle of vision of 2 degrees and standard illuminant D65. The colorimetric measurements were carried out only on the mock-up samples, not on the pigment powders. For each sample 4 up to 6 measurements were performed.

3.2.6 Scanning electron microscopy coupled with energy dispersive X-ray spectrometry (SEM-EDX)

A scanning electron microscope is a type of microscope that permits to obtain high resolution tridimensional images magnified more than 100,000 times due to the use of high energy electrons, typically in the range of 5 to 25 keV. The surface area of the sample is scanned in a raster-like pattern by a focused electron beam, generating a point-by-point reconstruction. In this process multiple signals are produced but mainly two are use to built up the image: secondary electrons (low energy, <50eV)

and primary electrons that are also elastically scattered by the sample material and scattered back from the sample to the detector. The higher the atomic number of the specimen atoms, the stronger the scattering and the more backscattered electrons that reach the detector. While secondary electrons give information about the morphology of the surface, backscattered electrons give information about the variation of chemical composition in the sample. The image is built up in a grey-scale where the brightness is function of the atomic number of the elements. The SEM used was coupled to an X-ray detector for the acquisition of detailed elemental information[17].

SEM-EDX was used to observe the cross-sections after degradation experiments in order to check if a degradation layer was formed. Additionally also elemental mapping and EDX point measurements were performed.

The samples were examined with a Field Emission Gun – Environmental Scanning Electron Microscope (FEG-ESEM) equipped with an Energy Dispersive X-Ray (EDX) detector (FEI Quanta 250, USA; at AXES and EMAT research groups, University of Antwerp), using an accelerating voltage of 20kV, a take-off angle of 30°, a working distance of 10 mm and a sample chamber pressure of 10-4 Pa. Imaging was performed based upon secondary electrons (SE), back-scattered electrons (BSE) and characteristic X-rays (EDX). For the latter elemental distribution maps (Sample1: 50 frames, Sample 6: 102 frames) were recorded with a beam current of ~0.3 nA at a magnification 1500x (Sample1) and 2000x (Sample6), a resolution of 512x352, and a dwell time of 100 μs per pixel, resulting in a total scan duration between 3000 – 4000s. EDX point spectra were acquired, using a beam current of ~0.3 nA and a dwell time of 30 s per spectrum. All the surfaces examined were previously coated with a thin carbon layer in order to obtain a conductive surface.

3.3.7 X-ray powder diffraction (XRPD)

X-ray diffraction is a rapid analytical technique primarily used to obtain information about the crystallographic structure of a material. XRD is based on constructive interference of monochromatic X-rays and a crystalline sample. X-rays are directed toward the sample with a θ angle and when conditions satisfy the Bragg's Law ($n\lambda = 2d \sin\theta$) the interaction between the incident rays and the sample

produces constructive interference (and a diffracted ray). The X-rays are diffracted at specific angles from each set of lattice planes in the sample. Because each crystalline material has a characteristic atomic structure, it will diffract X-rays in a unique characteristic pattern. The diffraction peaks (depending from 2θ) can be converted to d-spacing allowing the identification of the material by comparison of d-spacing standard reference patterns[41]. When applied to cultural heritage artifacts, reflection-XRPD allows the identification of crystalline pigments, and since it is a surface-sensitive technique is useful in the detection of surface degradation products.

Initially XRD was used to characterize the pigment powders and the commercial paint and have a better insight of their crystal structure. After degradation experiments this technique was used on the mock-up samples in order to identify possible degradation products.

The instrument used for analyzing the samples for this thesis is non-invasive prototype macroscopic X-ray powder diffraction scanning device employed in reflection-mode (AXES Research Group, University of Antwerp, Belgium). A scheme of the XRD set-up is given in Fig.14.

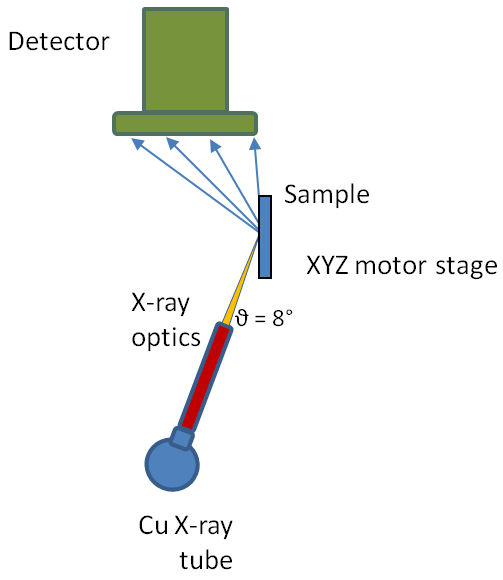

Fig.14 – Reflection XRD set-up

To generate the X-ray beam an Incoatec microfocus X-ray source (Cu-K_α X-ray tube, energy = 8.047 keV) coupled to a high voltage generator, was used. The X-ray source is equipped with Montel optics, consisting of two Göbel mirrors arranged in a

90° side-by-side geometry, which focuses the X-ray beam in both dimensions. The incident angle (θ) was 8° and the spot size (h x v) 1x0.15 mm^2. The samples were attached to a sample holder and mounted on top of a set of three motor stages (Newport corp.) which allow the sample to be moved in the X, Y and Z direction. During the scanning operation, the sample is moved in the X (maximum range: 100 mm) and Y (maximum range: 250 mm) directions, while the Z stage allows the positioning of the focal point of the X-ray beam on the desired part of the sample. For detection of the diffracted X-rays a Pilatus 200K (Dectris), a two-dimensional hybrid pixel array detector (HPAD), was used.

The in-house developed software package XRDUA was used for data processing. XRDUA provides the necessary tools for extracting crystalline-specific distributions from the large number of 2D diffraction patterns obtained during XRPD imaging experiments. Using reference files from the PDF-2 and COD database various crystalline phases present in the samples could be identified. In the diffractograms obtained the Q-space (1/nm) is a energy independent parameter where $Q = 2\pi/d$. The instrumental parameters employed are the same for all samples:

- Voltage: 50 kV
- Current: 1 mA
- Exposure time: 10 s/pt

4. Results and discussion

4.1 Characterization of the pigments

In order to have a complete overview of the elemental composition and crystal structure of the pigments studied in this thesis, μ-Raman spectroscopy, X-ray diffraction and XRF were used. Colorimetric measurement were carried out to describe the hue of the three colors and to monitor their color variation after degradation experiments.

4.1.1 XRF analysis

A preliminary elemental analysis was carried out by XRF. As expected, LAY ($Pb_2Sb_2O_7$) contains lead and antimony, while LTAY ($Pb_2SnSbO_{6,5}$) contains lead, antimony and tin. In the Naples yellow pigment powder that was analyzed the ratio Sb-L:Pb-L is 0.054, while for the lead-tin-antimony yellow the ratio Sb-L:Pb-L is 0.018, indicating that in the first one there is an amount of antimony of three times more than in the second one. With regard to the commercial Naples yellow (NG), although it is supposed to contain just pure lead antimonate, as declared by the manufacturer, XRF measurements show that, in addition to lead and antimony, also tin and aluminum are present (Fig.15).

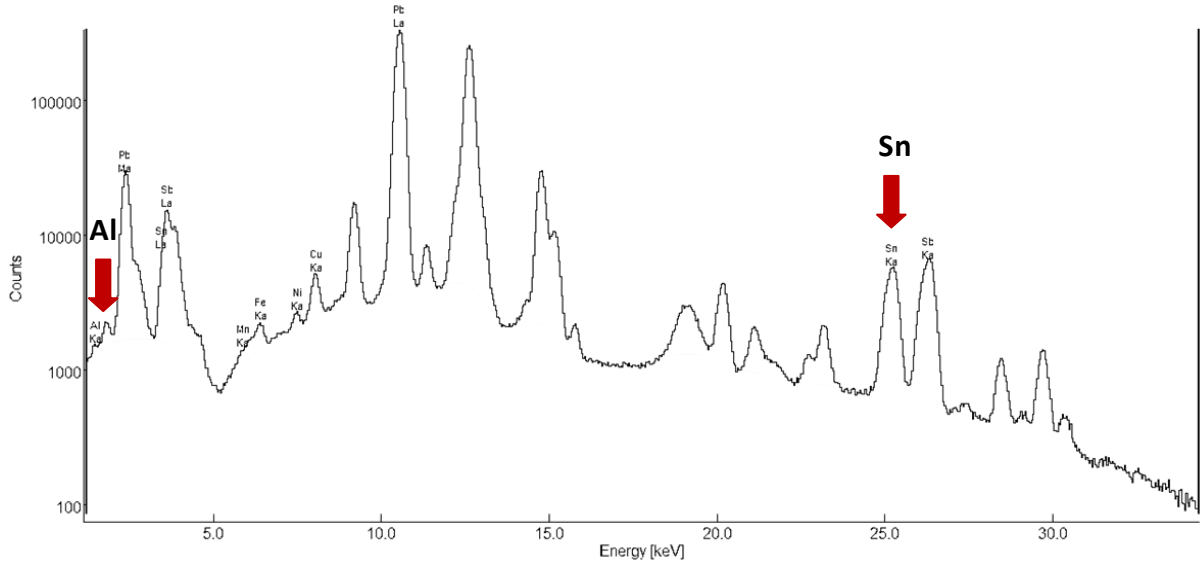

Fig.15 - XRF spectrum of NG

4.1.2 Raman analysis

As presented in Chapter 1 (*par. 1.2.2*) Naples yellow and lead-tin-antimony yellow have a cubic pyrochlore structure with the difference that, in the latter, also tin is present in the crystal lattice. Is known from literature[11,16,42] that the introduction of a third cation in the binary structure of lead antimonate ($Pb_2Sb_2O_7$) strongly affects the Raman vibrational spectra of this pigment due to a deformation of the pyrochlore structure to which Raman spectroscopy is very sensitive. Indeed the two pigments are well discernible with this technique[11,42].The Raman scattering features obtained for the three pigments considered in this study are presented in Table 1 and are in good agreement with the ones from literature[10,11, 42,43].

Table 1 - Raman bands of the analyzed pigments (red laser, λ=785 nm)

Sample	**Pigment**	**Chemical formula**	**Wavenumber (cm^{-1})***
LAY (powder)	Naples yellow	$Pb_2Sb_2O_7$	128vw, 198m, 228m, 298m(br), 348w, 394w, **504vs**, 794w(br)
LTAY (powder)	Lead-tin-antimony yellow	$Pb_2SnSbO_{6,5}$	**139vs**, 298w, **337s**, 450w, 508m, 775w(br)
NG (paint)	Genuine Naples yellow dark PY41	$Pb_3(SbO_4)_3$ or $Pb(SbO_3)_2$**	**140vs**, 302w, 342m, 459w, 507m, 755w(br)***

*vs=very strong, s=strong, m=medium, w=weak, vw=very weak, (br)=broad
**as reported in the Colour Index
***bands of the binding medium are not considered

As shown in Fig.16 (a) LAY has a strong fluorescence starting from 1000 cm^{-1} circa. Measurements, carried out with a red laser (785 nm), were repeated on several spots and in all the spectra collected fluorescence could be observed. In order to check if fluorescence could be reduced laser wavelength was changes and the green laser (514.5 nm) was used, but with no results. Probably the fluorescence is due to impurities present in the pigment itself. Anyways, since the peaks characteristic of the pigment lie between 100 and 800 cm^{-1}, they were visible despite the fluorescence. Therefore the following spectra were recorded in the range 100-800 cm^{-1}.

In Fig.16 (b) LAY spectrum in the range between 100 and 1000 cm^{-1} is shown. LAY presents the most intense scattering peak at about 510 cm^{-1} that can be ascribed to the totally symmetric elongation of the SbO_6 octahedra (A_{1g} mode). In the lower

spectral range (100-300 cm^{-1}) the bands are assigned to the Pb_4O tetrahedral vibrations; between 110 and 147 cm^{-1} a strong band attributed to a lattice Pb-O stretching mode is expected but it's not observed in the LAY spectrum because of the cut-off of the instrument used. The peak visible at 298 cm^{-1} could be attributed to the vibrational mode F_{2g} while the peak at 348 cm^{-1} to the vibrational mode E_g, both related to Sb-O and Pb-O bonds. The band at 794 cm^{-1} does not have an unequivocal assignment[11].

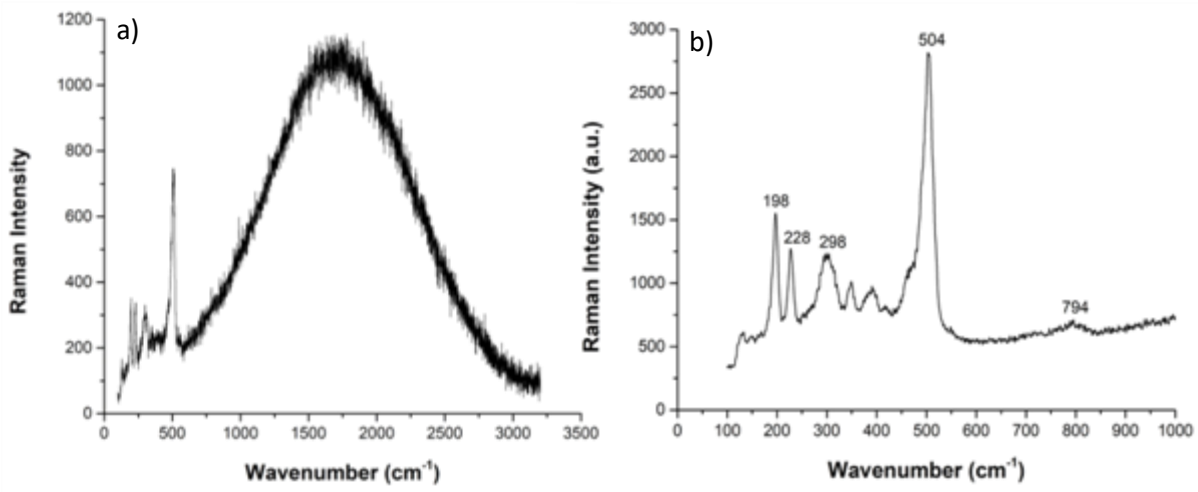

Fig.16 – Raman spectrum of LAY in the range 100-3200 cm^{-1} (a) and in the range 100-1000 cm^{-1} (b) (red laser, 0,1%)

The two bands at 198 and 228 cm^{-1} have not been identified but, as reported by some authors, additional bands in the Raman spectrum of lead pyroantimonates might be related to a disorder-induced symmetry lowering due to distortion of the SbO_6 octahedra or displacement of the Pb cations[11]. Agresti *et al.*[43] report that the bands between 180 and 230 cm^{-1} could be ascribed to Cl-Pb-Cl bond suggesting the formation of compounds where the two elements are associated. The possible presence of Cl is connected to the use of NaCl as a flux agent in the calcination process.

Analyzing different grains of the Naples yellow powder it was noticed that the ratio between the intensities of the peak at 198 cm^{-1} and the one at 228 cm^{-1} changes. In particular, as illustrated in Fig.17, in the spectra (a, b, c, d) where the peak at 198 cm^{-1} shows a higher intensity than the peak at 228 cm^{-1}, the main band at 512 cm^{-1} is shifted to a lower value (500 cm^{-1}), it decreases and become broader. Additionally a shoulder at around 455 cm^{-1} appears. The fact that spectra with different features are

obtained from the same sample suggests that the pigment powder is not homogeneous; two or more phases of $Pb_2Sb_2O_7$ with different molar ratio of Pb and Sb might be present. Indeed, a similar behavior was reported by *Rosi et al.*[11] while studying the influence of different molar ratio (Pb:Sb) in lead antimonates. They showed that an excess of Pb entails a decrease of the peak at around 510 cm^{-1} combined with the increase of a peak at around 460 cm^{-1}. So, this might be the case also for the Naples yellow analyzed in this study (see XRD results).

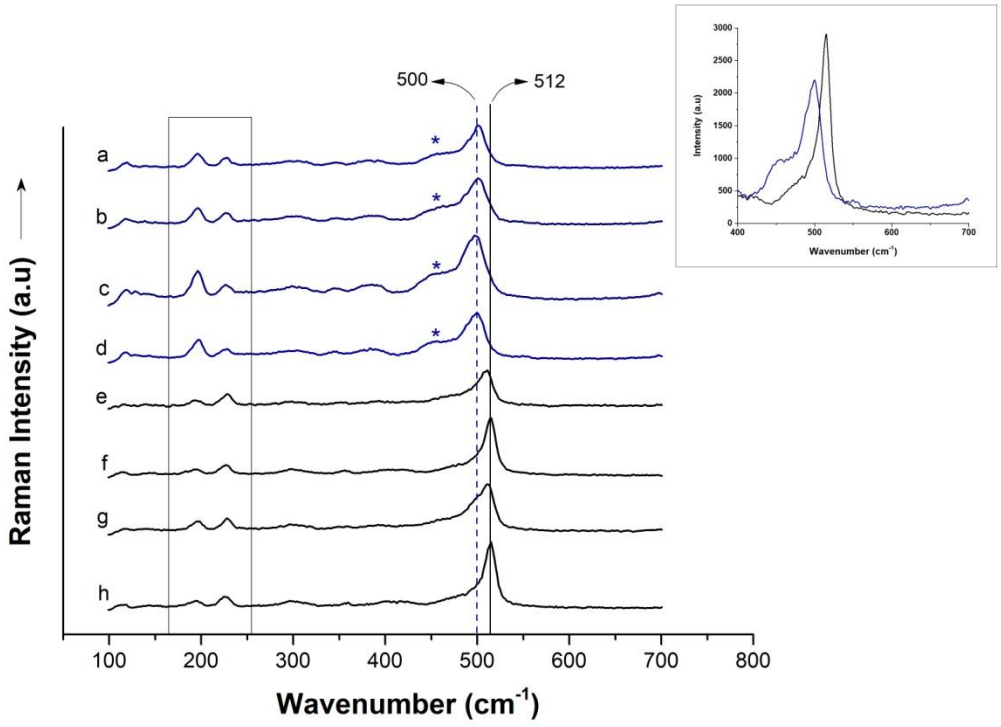

Fig.17 – Micro-Raman spectra collected from different grains of the Naples yellow powder. Inset: enlarged view of the main band at around 510 cm^{-1} of spectra (h) and (d) showing the different intensity (green laser, 0,5%)

On the contrary of Naples yellow, lead-tin-antimony yellow does not show any difference in the spectra depending on the point of analysis and neither shows fluorescence. Repetition of Raman measurements on different grains of LTAY pigment powder presented the same spectral pattern, as shown in Fig.18 – b.

As discussed before, is known from literature that lead-tin-antimony yellow is well discernible from Naples yellow with Raman spectroscopy. Indeed, in Fig.18 a comparison between Raman spectra of Naples yellow (a) and lead-tin-antimony

yellow (b) is presented. In this figure are evident the differences in the spectrum introduced by the presence of tin.

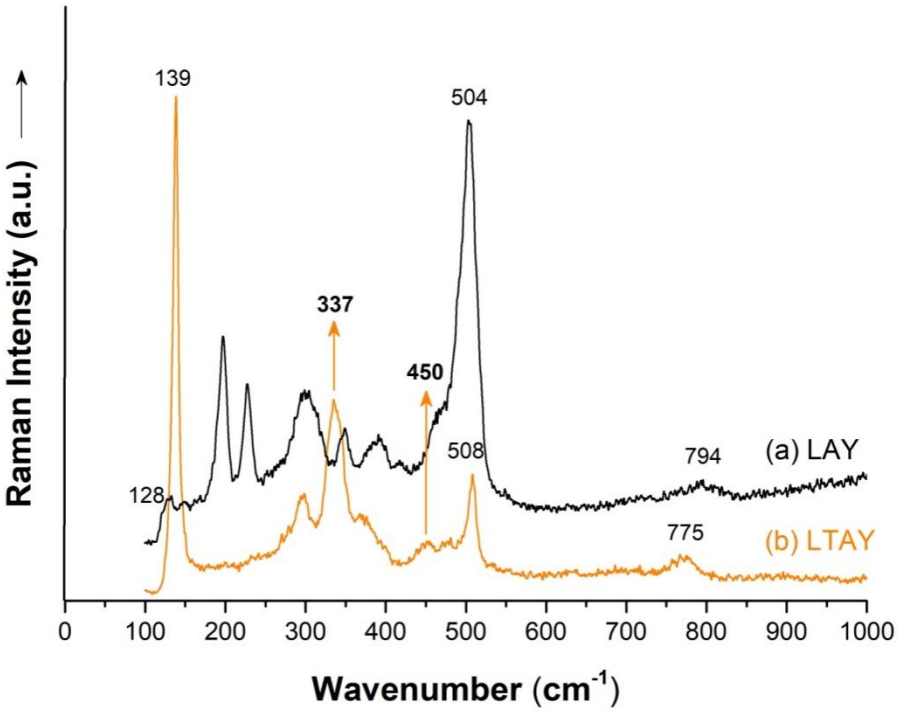

Fig.18 – Comparison between Raman spectra of Naples yellow (a) and lead-tin-antimony yellow (b) pigment powders (red laser, 0,1%)

The band in the lower spectral range assigned to a lattice Pb-O stretching mode, which is not visible in the LAY spectrum, is shifted towards higher wavenumbers (139 cm^{-1}) and appears as a intense and sharp peak.

The bands involving the more rigid Sb-O bonds of the octahedral network are very sensitive to any variation in the pyrochlore structure, reflecting strong changes in the spectra. It can be observed that there is a clear increase of the band at 337 cm^{-1} (Sb-O and Pb-O modes) which is characteristic for ternary compounds, but the most important modification in the spectra ascribed to the introduction of tin in the crystalline structure is the collapse of the band at around 510 cm^{-1} (A_{1g} mode, totally symmetric elongation of the SbO_6 octahedra) accompanied by the appearance of the band at 450 cm^{-1}, indicative of the modified pyrochlore structure. The unassigned signal at 794 cm^{-1} in the lead antimonate spectrum is red-shifted to 775 cm^{-1} for the lead-tin-antimony yellow.

In Fig.19 it can be observed that Raman spectra of the commercial Naples yellow (NG), look almost identical to the one of LTAY, having the same bands with a slight

shift in the wavenumbers (see Table 1). Since the commercial paint is supposed to be pure lead antimonate, it was expected to have Raman spectra with scattering features comparable to LAY. Instead, Raman measurements suggest that the pigment contained in NG has a crystalline structure similar to lead-tin-antimony yellow. This result indicates that the pigment is a pyrochlore with a third cation in the crystal lattice (discussed before for LTAY). As previously pointed out by the XRF analysis the commercial Naples yellow contains also tin that, considering these results, turned out to be not just an impurity in the paint but part of the crystalline structure of the pigment. After these consideration, NG should be called lead-tin-antimony yellow, rather than Naples yellow.

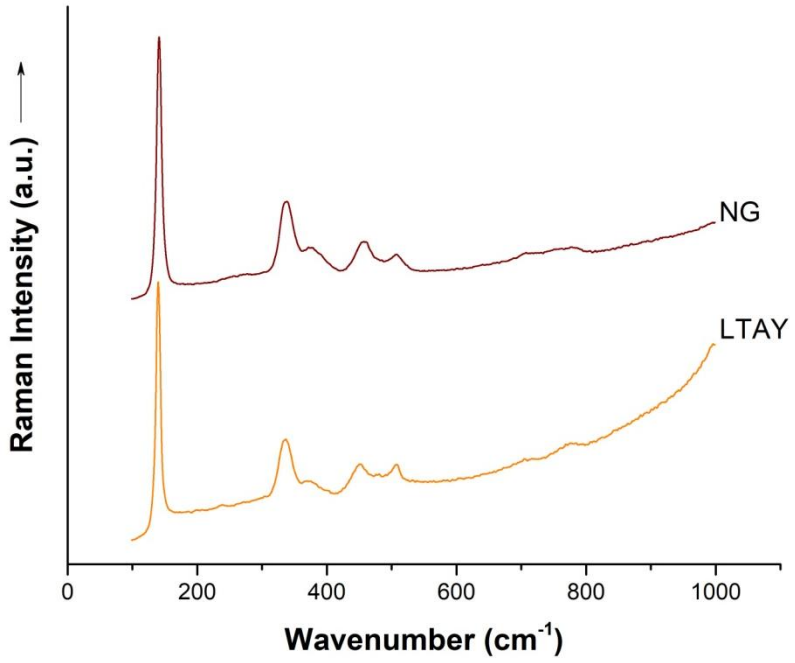

Fig.19 – Comparison between Raman spectra of $Pb_2SbSnO_{6.5}$ (LTAY) and the commercial Naples yellow (NG). (Green laser, 5%)

4.1.3 XRD analysis

The diffractogram of LAY (Fig.20) shows that the pigment's diffraction lines correspond to the bindheimite ($Pb_2Sb_2O_7$) lines, which is the isostructural analogue mineral of the pigment. The space group is Fd3m, that corresponds to a cubic pyrochlore structure. Hexagonal and orthorhombic $Pb_2Sb_2O_7$ phases might be present

as well. Moreover also traces of PbO (litharge) and/or minor unknown products were detected.

It's interesting to notice that the main diffraction peaks relative to $Pb_2Sb_2O_7$ are split into two separate maxima (Fig.20). According to Dik *et al.*[1] the splitting of the peaks can be attributed to the presence of two phases of lead antimony yellow with slightly different unit cells (suggesting different ratio of Pb and Sb). They suggest that this behavior is caused by the low temperature (650 °C) used during the preparation process. The presence of more than one phase of lead antimony yellow indicated by XRD measurements is in agreement with Raman results, which, as seen before, also suggest the presence of a non homogeneous pigment powder. However, the pigment analyzed in this work was synthesized at 800 °C, a much higher temperature than 650 °C. This observation opens another question about the origin of such split, which remain to be clarified.

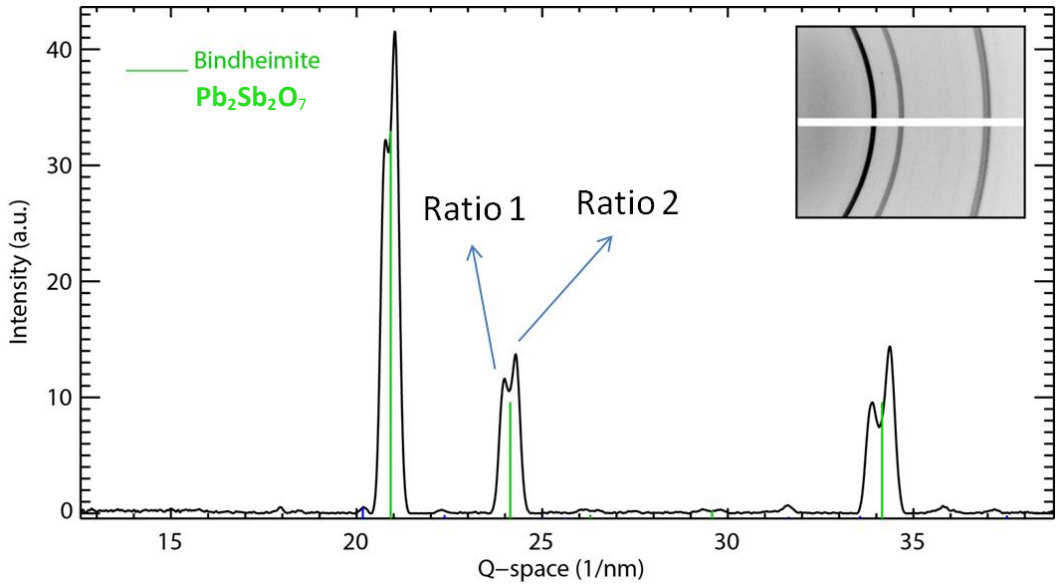

Fig.20 - Diffractogram of lead antimony yellow pigment powder (LAY) where the splitting of the peaks can be observed.

According to XRD results LTAY contains $Pb_2SnSbO_{6.5}$ as major product, confirming Raman data. Contrary to Naples yellow, this pigment presents sharp peaks and no splitting is observed (Fig.21 – a), suggesting a more homogeneous composition, in agreement with Raman analysis. The presence of a small quantity of SnO_2,

cassiterite (Fig.21 – b) seems to be common in lead-tin-antimony yellows and can be ascribed to the incomplete reaction of the starting materials[9].

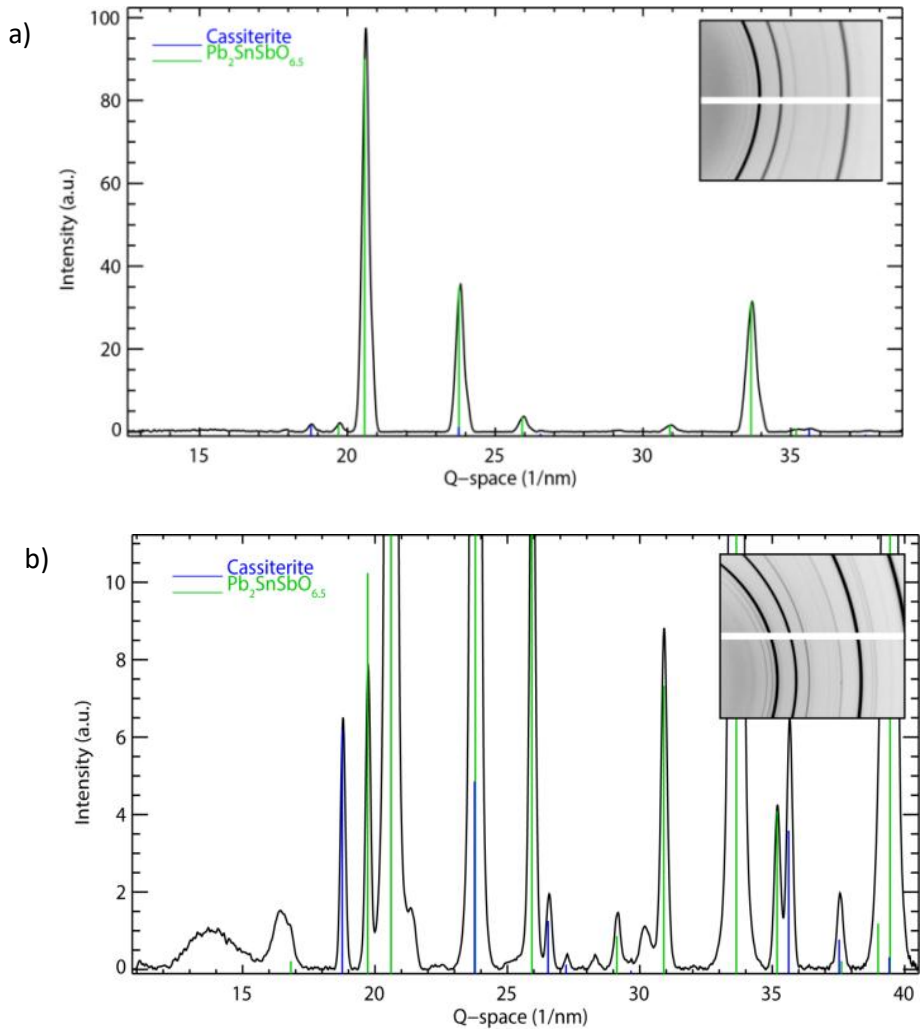

Fig.21 – Diffractogram of LTAY pigment powder (a) and a zoom in showing the peaks of SnO_2 (b)

In the sample NG, the commercial Naples yellow, bindheimite ($Pb_2Sb_2O_7$) turned out to be the dominant phase. Also the organic binding medium (linseed oil) was detected and possibly other minor compounds, that were not identified, are present. In Fig.22 the diffractogram of NG is reported.

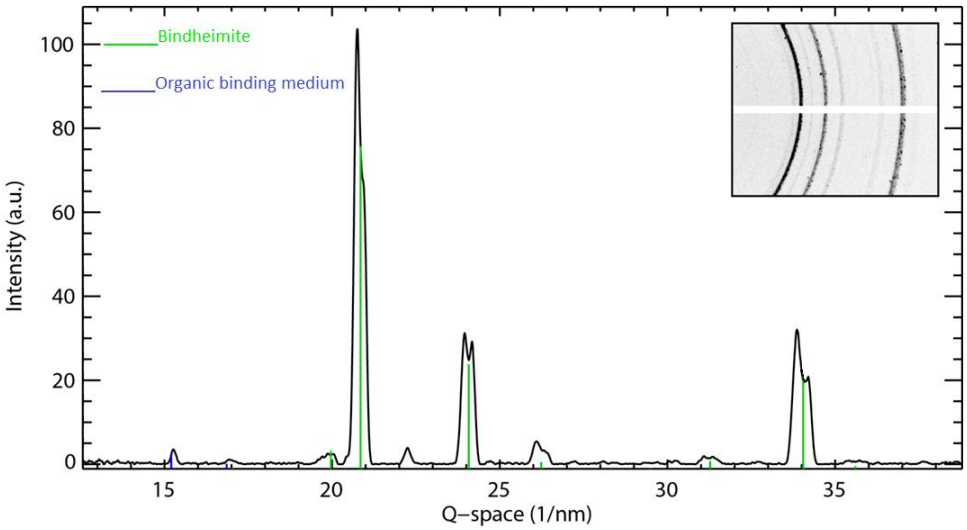

Fig.22 – Diffractogram of the commercial Naples yellow (NG)

Although the manufacturer claimed that their Naples Yellow consists of pure lead antimonate, the diffraction experiments carried out on the paint showed that NG do not consist of cubic $Pb_2Sb_2O_7$ only. As seen before for LAY, also the peaks of NG are split indicating that two different phases of $Pb_2Sb_2O_7$ with different ratios of Pb and Sb might be present. The temperature of the calcinations process for this pigment is unknown, so it is not possible to understand if that is the origin of such split. As underlined by Dik *et al.*[44] even 20th century industrially produced Naples yellow cannot be consider a pure a pure cubic $Pb_2Sb_2O_7$ phase. Other phases can be present as well, be it as intentional adulteration or as unintentional by-products of the production process.

Interestingly XRD measurements are in contrast to what shown before by previous analysis. Indeed, Raman analysis, in accordance with XRF analysis, showed that NG contains tin and has a crystalline structure more similar to lead-tin-antimony yellow rather than Naples yellow, the opposite of what shown by XRD. Further studies need to be done to better understand the composition of this pigment.

4.1.4 Colorimetric measurements

To complete the characterization of the pigments, colorimetric measurements were carried out. In Table 2 the colorimetric parameters L*(lightness), a*(red-green)

and b*(yellow-blue) are reported and in Fig.23 the three colors are represented in the color plane. The values for each color are an average of six measurements.

Table 2 – Colorimetric parameters

	L*	a*	b*
LAY	89.98	1.24	62.26
LTAY	83.02	4.93	53.94
NG	80.71	7.80	55.65

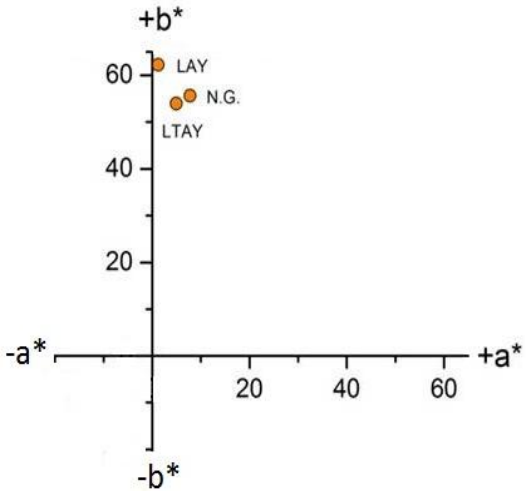

Fig.23 – Representation of the three colors in the a*-b* color plane

Naples yellow (LAY) is the brightest color with the highest yellow component (b*) and very low red component (a*). LTAY and NG have a more reddish hue and lower lightness (L*), with NG having the highest red component. It's interesting to notice that the commercial Naples yellow is more similar to lead-tin-antimony yellow also in the color hue, which was anyway visible also to the naked eye.

In literature there is no common agreement concerning the hue of the two pigments. Some authors[10,43,45], after synthesizing the pigments, describe Naples yellow as a warm yellow with a significant red coordinate in the CIE L*a*b* colour space (a* parameter between 6 and 19), while lead-tin-antimony yellow is reported to be a clear, brilliant yellow without reddish shades (a* parameter between 2 and 9) that made it unique with respect to yellow ochres. On the other hand Wainwright *et al*. define lead antimonate as a brilliant, light yellow, while according to Agresti[7] lead-tin-antimony yellow has a warmer hue (with orange tones) compared to other Pb-based pigments.

4.2 Naples yellow and lead-tin-antimony yellow: evaluation of their stability

4.2.1 Light-induced degradation

As mentioned in Chapter 1 recent studies[20,21]pointed out that some pigments, such as CdS, α-HgS, and chrome yellow, are semiconducting materials, so more prone to degrade towards light. In these studies a new approach was used based on photo-electrochemical experiments employed to investigate the mechanism of the degradation processes. This method allows to mimic a potentially harmful environment combing the effect of light (laser) with an electrolyte compound present in atmosphere (e.g. water-soluble salts, present in airborne particles, an organic acid etc.)[20]. By applying proper electrochemical methods it is possible to gather information about the degradation and monitor the processes in real-time. For example, by means of amperometry the photocurrent developed by the pigments under illumination can be measured, whereas additional information about the degradation products can be obtain by applying linear/cyclic sweep voltammetry.

A similar approach was adopted in this thesis work in order to check if the pigments considered in this study, Naples yellow and lead-tin-antimony yellow, are sensitive to light and might act as semiconductors materials. For the same purpose additional experiments with different lasers (green and blue) were carried out on mock-up samples and powders. Aging with UV light (climate chamber) was also tested. In addition preliminary DFT calculations helped to have a better insight of the electronic properties of the pigments.

Results of light-induced degradation are presented in this chapter.

4.2.1.1 Green laser experiment

A preliminary quick test to investigate the pigments sensitivity to light, was carried out employing the green (514.5 nm) laser of the Raman spectrometer. The experiment was performed both on the pigment powders (LAY and LTAY) and on the mock-up samples. The instrument allows to record a certain number of acquisitions on the same spot of the sample giving a spectrum for each acquisition. In this way it is possible to analyze the different spectra and check if the laser is degrading the pigment. For this study 10 acquisitions of 60 seconds each were taken on the samples of interest. The laser power was set at 5%.

First, the pigment powders (LAY and LTAY) were analyzed. It is assumed that, if the laser is degrading the pigments, a change in the Raman scattering features should be observed during the repetitions. In Fig.24 – a, spectra of LTAY pigment are presented (only the first and last spectrum of the repetitions are reported). It can be noticed that the spectrum acquired during the first measurement (1 – black line) and the last spectrum acquired (10 - orange dash line) are perfectly overlapped indicating that the laser did not have any effect on the pigment. A similar situation is observable for the Naples yellow pigment (Fig.24 – b), but in this case a slight decrease, in particular of the bands at 198, 228 and 510 nm, occurred. Further experiments are necessary to verify if the decrease always occurs under this conditions and if it can be related to the green laser illumination.

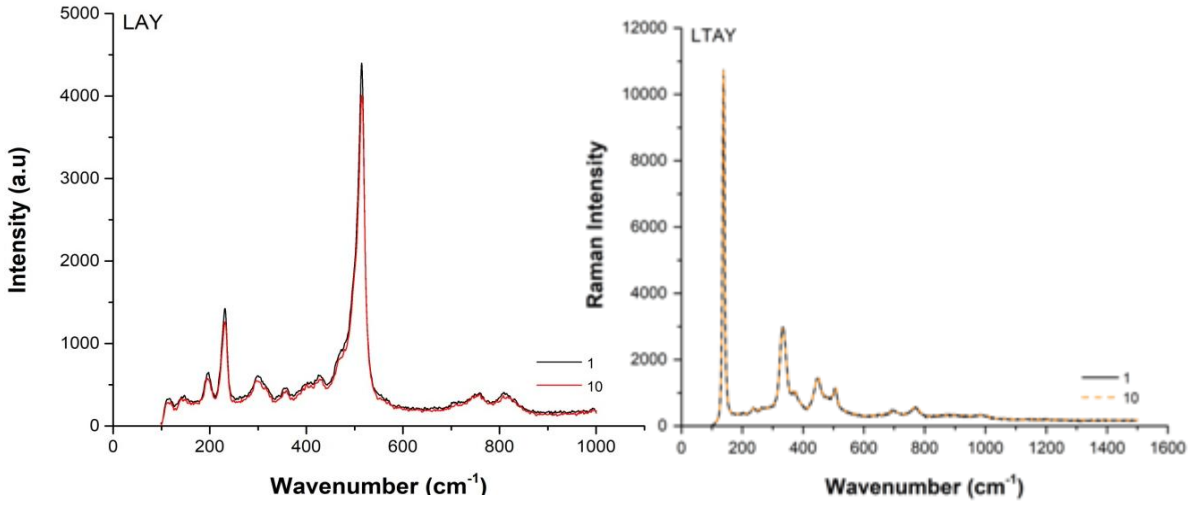

Fig.24 – First and last spectrum of the ten repetitions on the same spot with the green laser for LTAY (a) and LAY (b) pigments.

The same experiment was carried out on mock-up samples. No relevant changes were noticed for LAY or NG samples. Instead, concerning LTAY (Fig.25), it's interesting to notice that during the ten scans with the green laser on the same spot a progressive decrease of the background arises. The uppermost spectrum (1) exhibits a considerable fluorescent background whereas the lowest (10), which is the last scan out of the ten, shows a clear decrease of the rising background such that the peaks of the pigment are clearly more visible (Fig.25 – inset). Therefore it is assumed that irradiation lowers the level of the fluorescent background without altering the peaks of the pigment, which corresponds to an improvement in the signal to noise ratio of the Raman spectrum.

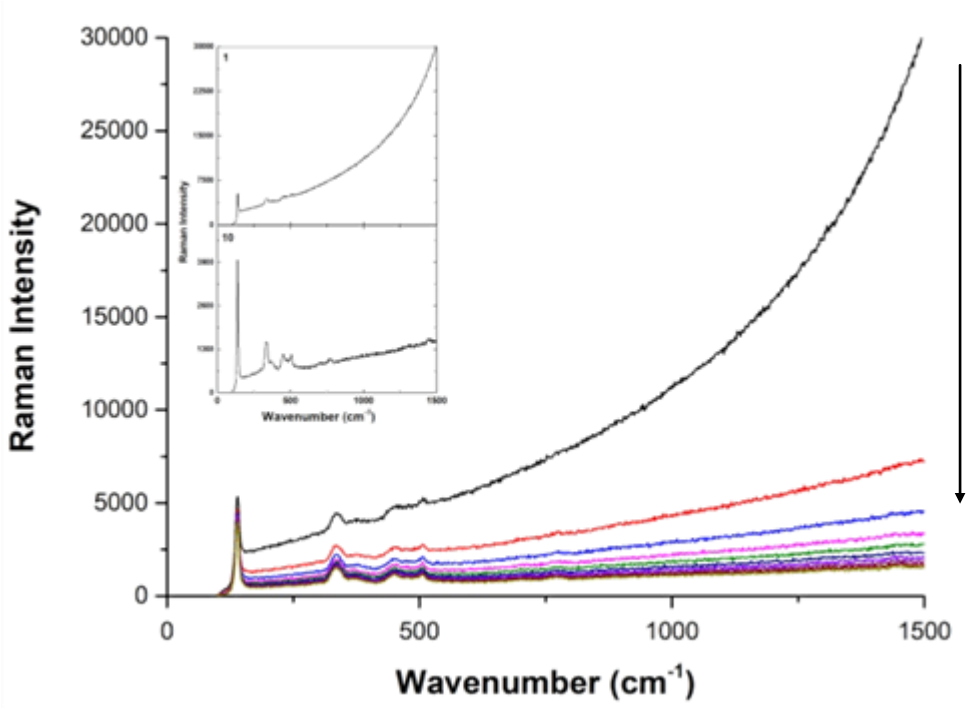

Fig.25 – 10 repetitions, 20s each with green laser at 5% on LTAY mock-up sample. Inset: first (1) and last (10) scan of the measurement

This trend suggested that a phenomenon similar to photo-bleaching was occurring. Photo-bleaching is actually a "technique" used in Raman spectroscopy to reduce the fluorescent background coming from a sample that often masks the characteristic peaks of the substance of interest. Indeed, photo-bleaching consists of irradiating the sample with intense light (the Raman spectrometer's laser) for a period of time after which spectra are acquired. The irradiation often induces a photolytic decomposition, breaking down the fluorescent molecules, hence reducing

the fluorescent background[46]. Fluorescence can be caused by a contamination of the surface (soiling) or by an organic substance present in the sample[47], that in this case is the linseed oil used as biding medium to produce the paints.

So, what is observed during the ten repetitions is a photo-bleaching of the binding medium, while the pigment stays unaltered. To confirm this, ten repetitions with the same parameters were carried out also on the pure linseed oil and as shown in Fig. 26 the same trend (progressive lowering of the spectra) is observed.

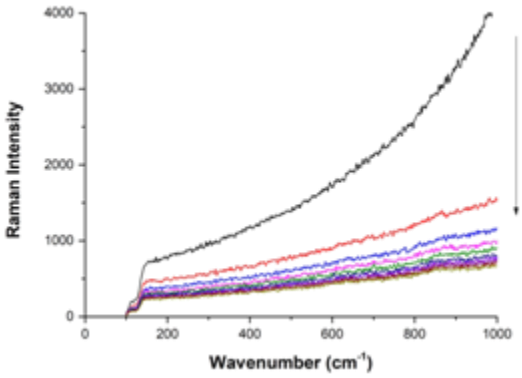

Fig.26 - 10 repetitions, 20s each with green laser at 5% on linseed oil

These considerations, even if they do not give information about the pigment's degradation, might be useful for future measurements, knowing that if a fluorescent background occurs, photo-bleaching of the sample can be used in order to lower the background and make the pigment peaks visible.

4.2.1.2 DR-UV-vis measurements and photo-electrochemistry

Since the green laser seems to have not much effect on the pigments (at least in the conditions used in this study), it was decided to have a deeper insight about the potential effect of light using a different (and more proper) approach by means of DR-UV-vis measurements and subsequently photo-electrochemistry.

In Fig.27 absorbance spectra of LAY and LTAY acquired by diffuse reflectance UV-Vis spectroscopy are presented. The spectra of both pigments show a clear absorption edge, which is considered a typical shape for semiconducting material[17] (the optical excitation of the electrons from the valence band to the conduction band is evidenced by an increase in the absorbance at a given wavelength (band gap

energy)[38]). In order to measure the band gap energy the linear section of the absorbance edge was taken and the corresponding absorption wavelength was determined and converted in E_g(eV). Results are summarized in Table 3. For Naples yellow the corresponding wavelength is 540 nm and the band gap 2,3 eV. Lead-tin-antimony yellow has a sharper absorption edge with a corresponding wavelength of 554,5 and a band gap of 2,24 eV, slightly lower than the one of LAY.

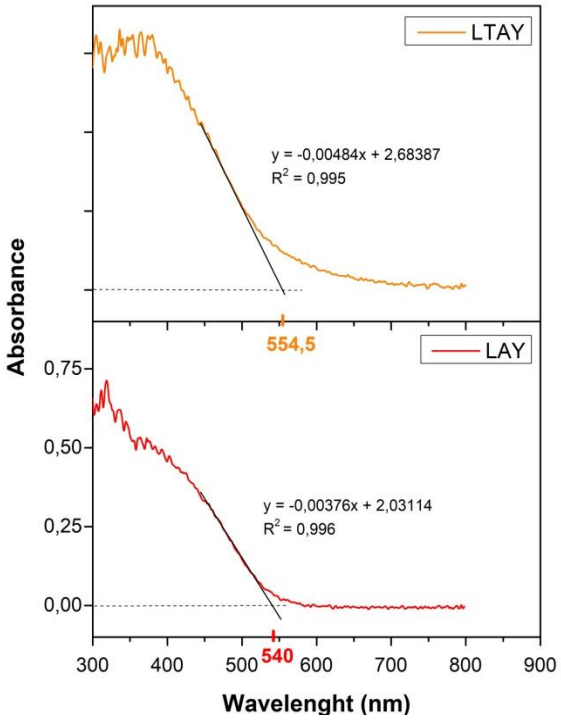

Fig.27 – DR-UV-vis measurements of $Pb_2SnSbO_{6,5}$ and $Pb_2Sb_2O_7$. The wavelength corresponding to the band gap energy is indicated.

Table 3 – Wavelength and relative band gap energy of the two pigments

Pigment	Wavelenght (nm)	Band gap (eV)
$Pb_2SnSbO_{6,5}$	554,5	**2,24**
$Pb_2Sb_2O_7$	540	**2,3**

$\lambda(nm) \leq 1241/E_g\,(eV)$

The band gaps values are relatively small and consistent with the color of the pigments. The Naples yellow is only excited with illumination of light with $\lambda \leq 540$ nm (E_g = 2.3 eV). Lead-tin-antimony yellow, on the other hand, having a lower band gap energy (E_g = 2.24 eV), allows electron excitation from $\lambda \leq 554,5$ nm. Previous studies[20,21] showed that semiconducting pigments such as CdS and $PbCrO_4$ have absorbance spectra with a clear absorption edge (an example is reported in Fig.28 for CdS) and a band gap energy of 2,4 eV and 2,2 eV, respectively, so very similar to the values calculated for the pigments in this study.

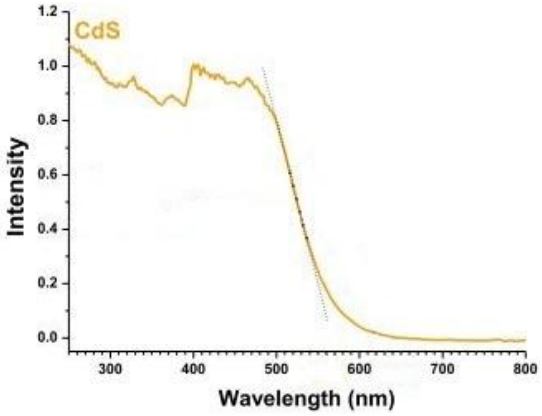

Fig.28 – DR-UV-Vis spectrum of CdS[17]

From these results, the hypothesis that Naples yellow and lead-tin-antimony yellow might be also semiconducting pigments was considered. Therefore the next step was to verify if under illumination the pigments were photo-active, hence a photocurrent could be measured. For the electrochemical experiments a laser with a supra band gap energy was chosen (blue laser – 405 nm) to make sure the light was fully absorbed by the pigments.

After deposition of a thin layer of lead-tin-antimony yellow (LTAY) on the working electrode OCP and amperometry with cycles of darkness and illumination were performed. The experiment was repeated for three different electrodes. Since the procedure of deposition does not allow the perfect control of the amount and distribution of the pigment on the electrode, the reproducibility was not perfect. The choice of the suspension concentration (50 mg pigment in 1 mL ethanol) for these experiments was based on previous studies[20] showing that it is the one with the lowest standard deviation.

In Fig.29 the OCP of LTAY is presented. A drop of potential is observed immediately after the laser was switched on. After illumination the OCP slowly stabilizes, but not completely. The OCP value is subsequently taken as the fixed potential in the amperometric experiment. In this way the electrode is near the equilibrium in the dark and the background is not influenced by any overpotential reaching a situation comparable to a "natural" environment[20].

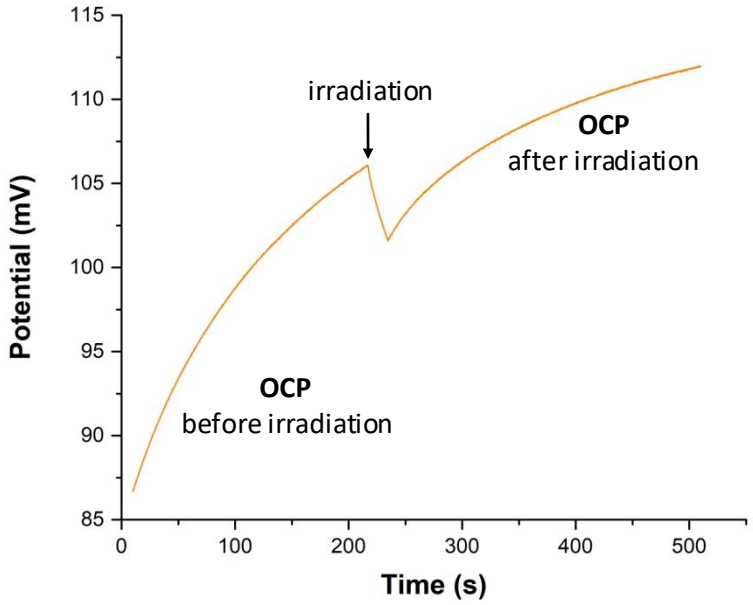

Fig.29 – Open circuit potential of LTAY before, during and after illumination with the blue laser

During amperometric measurements, five alternating cycles of darkness (~10s) and illumination (~30s) were applied. As shown in Fig.30 a raising in the current is clearly visible during the illumination cycles. The sign of the current indicates that electrons move externally from the WE to the CE, and thus that an oxidation occurs at the WE. Compared to previous studies[17]of semiconductor pigments, as CdS, following this approch to investigate the photoactivity of the pigments, the current measured for lead-tin-antimony yellow is definitively lower (less than 10 nA respect to hundreds of nA), but still discernible from the blank. Also in the blank oxidation peaks are visible during illumination, probably due to impurities on the electrode surface. Anyway, the photocurrent recorded after the deposition of the pigment is five time higher than the one revealed for the blank, indicating that the pigment is indeed developing a photocurrent. After each cycle the current measured is lower than the one measured for the cycle before.

These results indicate that the photocurrent comes from an oxidation process, however it's not clear which is the element involved in the process. A similar behavior was observed for lead chromates[21], but measurements in ionic liquid showed that the oxidation observed when using NaCl as electrolyte, was ascribed to the aqueous media and not to the pigment. A similar ionic liquid test with LTAY was performed and a oxidation process was still recorded. Further studies are necessary to clarify this behavior.

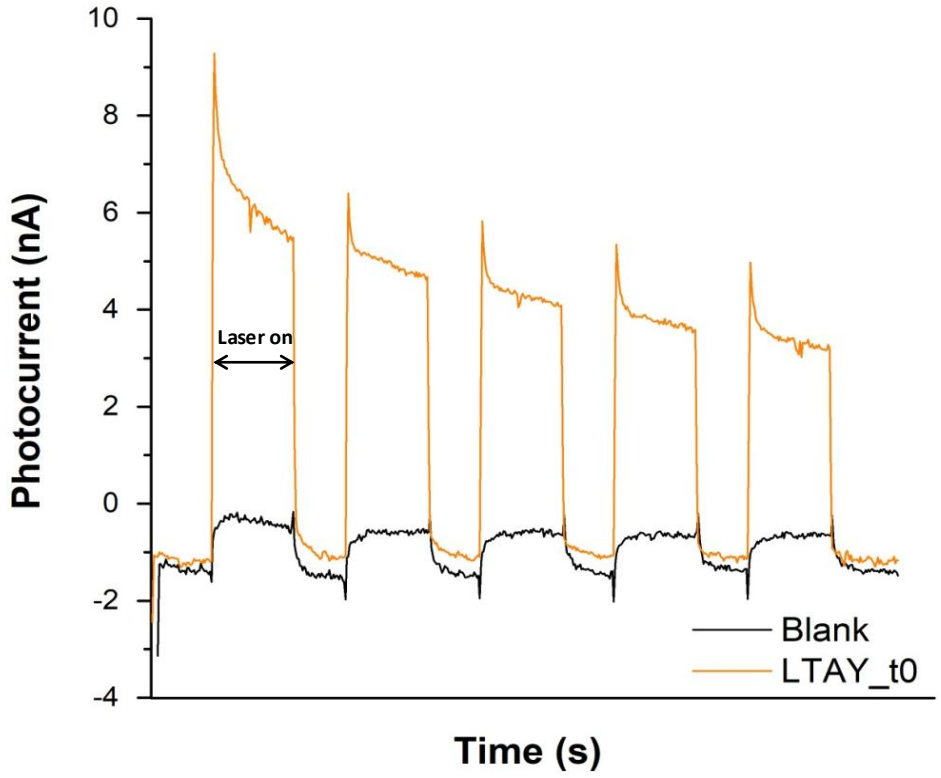

Fig.30 – Amperometry with alternating cycles of darkness and illumination of the blank (black line) and $Pb_2SbSnO_{6.5}$ (orange line) in 1 mM NaCl

The photocurrent is dependent on the amount of photosensitive material present on the electrode surface[17]. Therefore, the decrease in the photocurrent recorded after each cycle might be explained by the formation of a photo-degraded product which is not photoactive and/or water soluble.

After the experiment shown in Fig.30, where a decrease in the photocurrent was observed during the five cycles of illumination, further experiments were carried out illuminating the electrode for a certain time without any electrochemical intervention. Similarly to the previous measurements OCP was first determined and subsequently amperometry (with steps of darkness and illumination) was performed for other five times. In between every amperometric cycle the electrode was illuminated with the laser up to a total of 12 minutes irradiation (not counting the time of the illumination steps during the measurements). The sequence of amperometric measurements is shown in Fig.31. After longer periods of irradiation the photocurrent does not decrease at each step of illumination during amperometry, but it results almost constant.

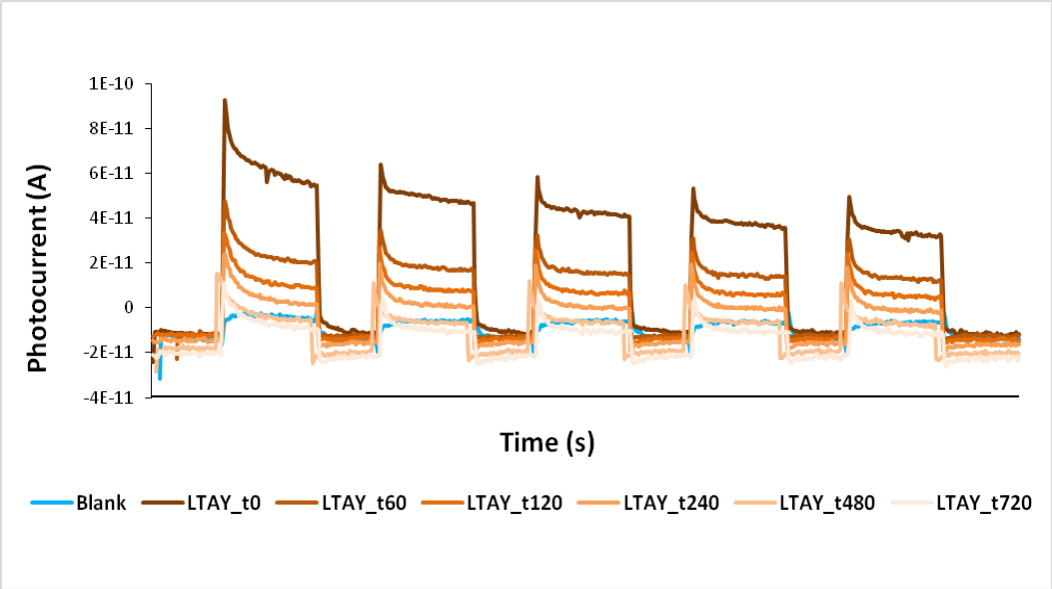

Fig. 31 – Cycles of amperometric measurements at increasing time of illumination

For each cycle of amperometric measurement the average photocurrent of the five steps of illumination was plotted against the different illumination times (Fig.32). With the increase of exposition time to the blue laser a clear decay in the photocurrent can be observed. The illumination somehow has an effect on the pigment and the final situation after 12 min exposition (below the limit of detection) is clearly different compared to the beginning. These results are in agreement with the hypothesis that a non-photoactive degradation product might formed due to illumination.

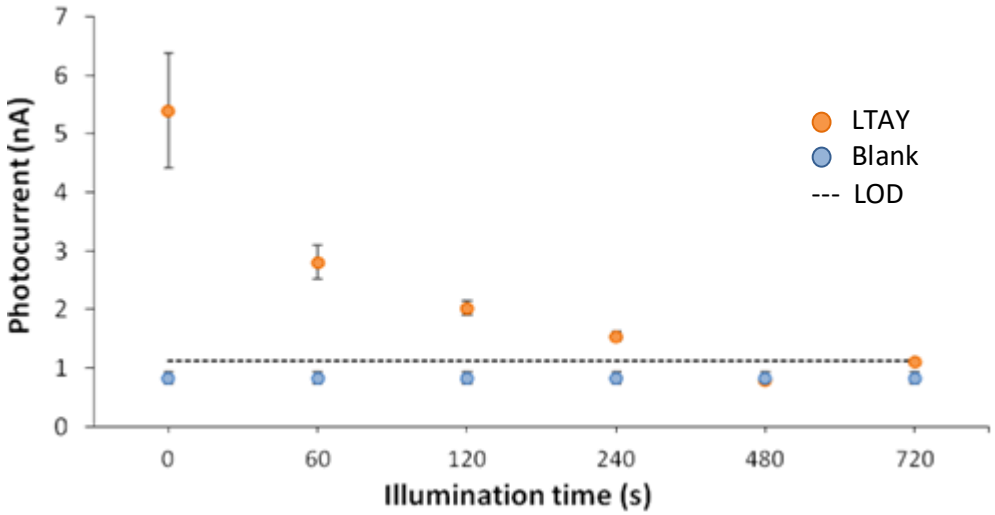

Fig.32 - Average photocurrent of the five cycles of illumination measured during amperometry plotted against the relative illumination time.

Concerning Naples yellow (LAY) the same study were performed. During the open circuit potential measurement, when the laser was switched on, a small drop (~1mV) of the potential is observed (Fig.33 – a). After illumination the potential stabilizes. As explained before, the OCP was taken as the fixed potential for the amperometry. It's interesting to notice how Naples yellow, in the same conditions of $Pb_2SbSnO_{6.5}$, develops a much lower photocurrent (~1.5 nA) during the five cycles of irradiation with the blue laser (Fig.33 – b). As shown in Fig.33 – c, after prolonged illumination times up to 8 minutes, the photocurrent decays, as observed also for LTAY. However, it has to be noticed that the photocurrent relative to LAY is too low to consider the pigment photoactive. Indeed, the average photocurrent measured during the different amperometric experiments is barely above the limit of detection.

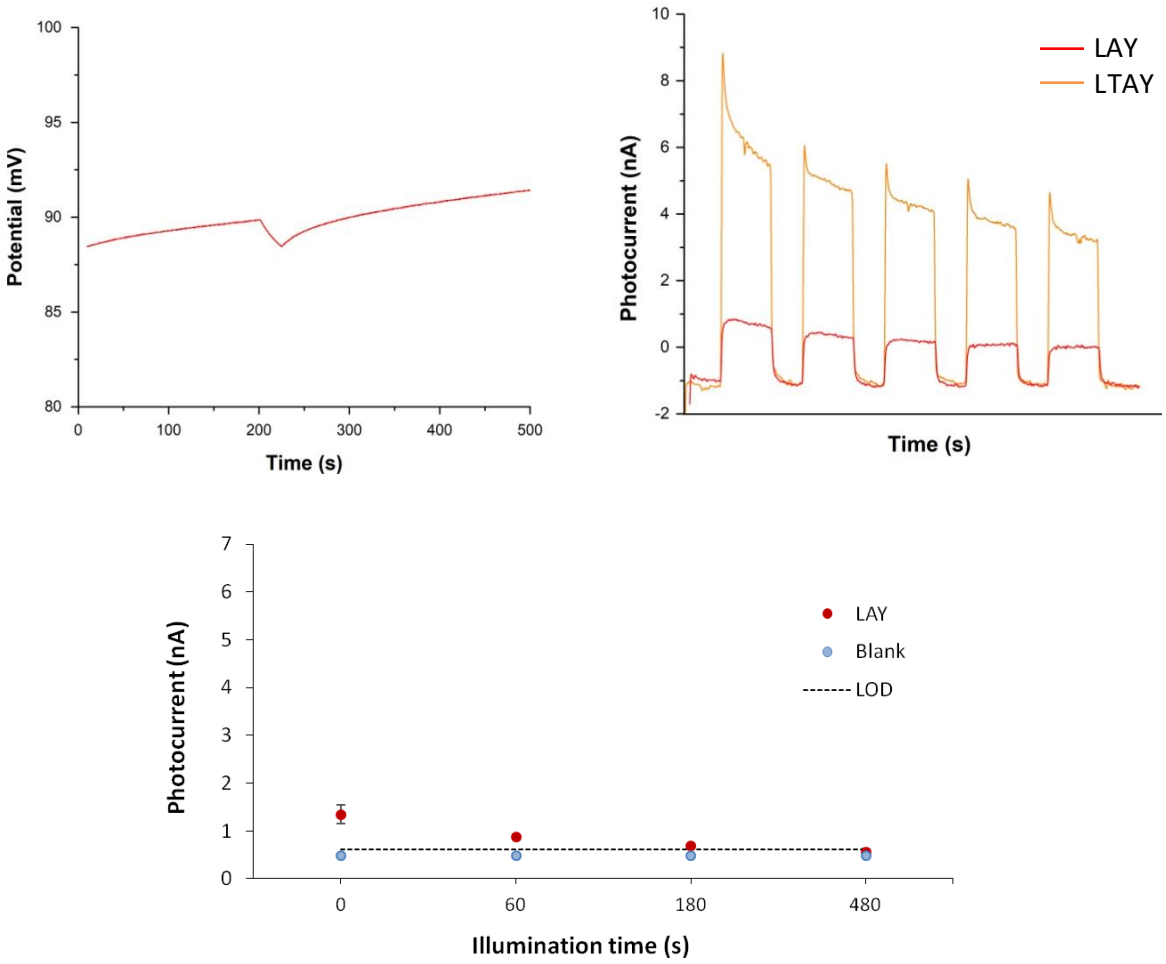

Fig.33 – G|$Pb_2Sb_2O_7$ electrode in 1mM NaCl. Open circuit potential (a), amperometry with alternating cycles of darkness and light (comparison with LTAY)(b), average photocurrent of the five cycles of illumination measured during amperometry plotted against the relative illumination times (c)

Photo-electrochemistry results indicate that the two pigments have different response to light irradiation. While lead-tin-antimony yellow is photo-active, Naples yellow shows a very low photocurrent, hence almost no photo-activity. Some consideration can be done about this behavior. Naples yellow and lead-tin-antimony yellow have the same crystalline structure (pyrochlore), but apparently tin has an influence in the photo-activity of the pigment. In a study about the photo-degradation of Chrome yellow ($PbCrO_4$) by Rahemi *et al.*[21] it was pointed out that lead chromate and its coprecipitates ($PbCr_{1-x}S_xO_4$) have a different photo-activity depending on the amount of sulfur present in the pigment. It was experimentally demostrated that under illumination with a blue laser light the photocurrent developed by the pigments increases with increasing S-content. These observations open a question if a similar behavior might occur also for Naples yellow ($Pb_2Sb_2O_7$) and lead-tin-antimony yellow ($Pb_2SnSbO_{6.5}$). And, in that case, how the presence in of tin influences the response to light of the pigments.

Further experiments are necessary to have a deeper insight of the photochemical behavior of these pigments. Moreover it would be worth to try different electrolytes in order to test if they might influence the photochemical response. Also the method of deposition of the pigments on the electrode should be improved to better control the amount and distribution of the pigment.

4.2.1.3 Blue laser experiment

Photo-electrochemistry could only be performed on pigment powders and for a relative limited time of illumination. So, in order to have a better insight of the pigments sensitivity to light, mock-up samples were illuminated for up certain time (up to 24 h) with a blue laser (405 nm, 50 mW) (Chap.3 - *3.2.1*). After irradiation, Raman measurements were carried out to evaluate the effect of irradiation on the pigments, or better, on the paints. In Fig.34 typical spectra of LTAY pigment before and after two hours irradiation are presented. The Raman spectra were acquired with a the red laser at a laser power of 1.17 mW corresponding to the 5% of the maximum laser power.

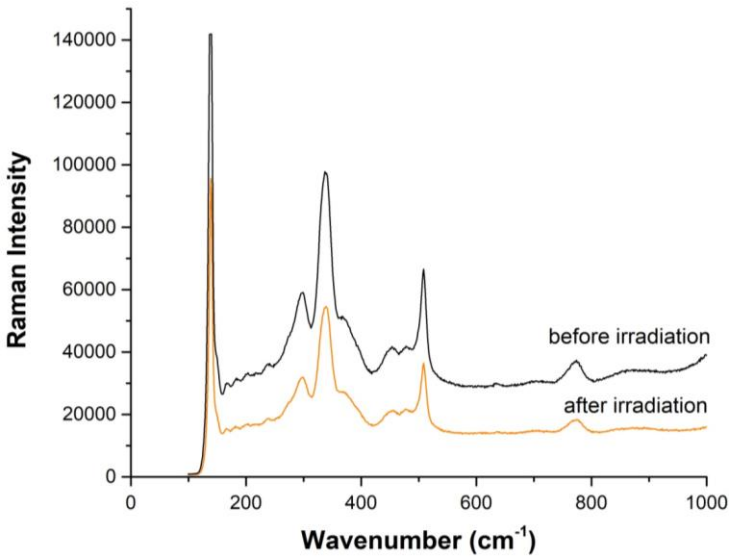

Fig.34 – Typical Raman spectra of LTAY before and after irradiation with a blue laser (red laser, 5%)

As shown in Fig.34, the background of the spectrum after irradiation decreases, suggesting that the binding medium (linseed oil) probably degraded. It was notice that after irradiation, spectra presented an overall decrease of the peaks which might be explained by a crystal structure modification. Further analysis need to be done to confirm that there is an actual decrease before and after irradiation.

The same measurement were carried out also for LAY. As shown in Fig.35, spectra obtained before (b) and after (a) irradiation are almost identical and no significant changes could be observed.

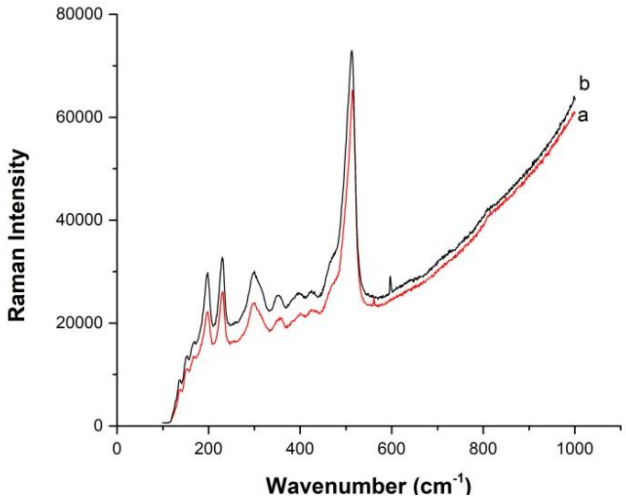

Fig.35 – Typical Raman spectra of LAY before and after irradiation with a blue laser (red laser, 5%)

Concerning the commercial Naples yellow (NG), since the begging it was noticed that Raman spectra obtained on it where quite different from each others indicating that the pain is probably heterogenous. Therefore, it was difficult to evaluate where the changes in the spectral pattern were due to the actual effect of illumination.

After 24h irradiation no additional results were observed compared to the 2h illumination.

4.2.1.4 Climate chamber (UV light)

A total of five mock-up samples for LAY (1,7,6,C,B), five samples for LTAY (1,7,6,C,B) and four samples for NG (1,7,6,E) were aged in the climate chamber for 1000 hours. After aging, samples were analyzed with Raman spectroscopy but no relevant results were obtained. Colorimetric measurements, instead, present some interesting results.

As explained in section *4.1.4 Colorimetric measurements,* mock-up samples prepared with the same paint present colorimetric values quite variable. For this reason it was decided to evaluate the change of the colorimetric parameters for each single sample instead of take an average for each group of samples (LAY, LTAY, NG). In order to evaluate the change in hue, a* was plotted against b* and the results are illustrated in Fig.36, 37 and 38 for LAY, LTAY and NG, respectively. The change in lightness (L*) is reported in Fig.39, while the total color change (ΔE) is represented in Fig. 40.

Concerning LAY samples, the major change is a decrease in the b* coordinate (yellow) together with a clear lowering of lightness (L*), while no significant shifts of a* (blue-red) occurred. Sample C is different from the others; it shows a desaturation of the color, but no changes of the hue(C before and C after lie on the same radius) and the lightness increases. So, except for sample C, all the other samples show the same trend after exposition to UV light. .

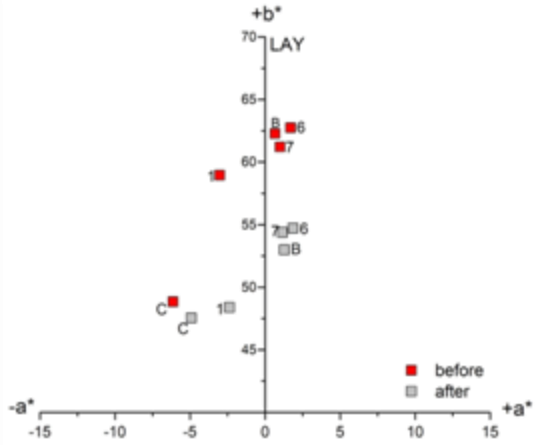

Fig.36 – a*-b* parameters of LAY samples before (red squares) and after (grey squares) UV light aging

LTAY samples (Fig.37) show a slight increase towards yellow (b*) accompanied by a small decrease in the red component (a*). Also for these samples a common trend can be observed. However, it has to be considered that measurements on the samples presents a relative high standard deviation compared to the small shift observed before and after irradiation. Therefore attention should be paid in the data interpretation. Regarding L* parameter, sample B, 6 and 7 show a modest decrease of lightness, whereas C and 1 show an increment.

Conversely to LAY and LTAY, NG samples do not show any specific trend. Samples 6 and 7 show a main decrease of b* and L*, while sample E an increase in the yellow component and in lightness. All the three samples show also a small decrease in the red component. For sample 1 a slight decrease of a* and an increase of L* is visible. On the whole, it is not possible to evaluate a change in hue for NG samples.

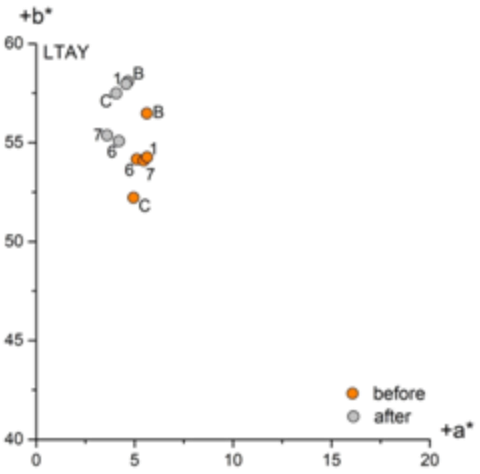

Fig.37 – a*-b* parameters for LTAY

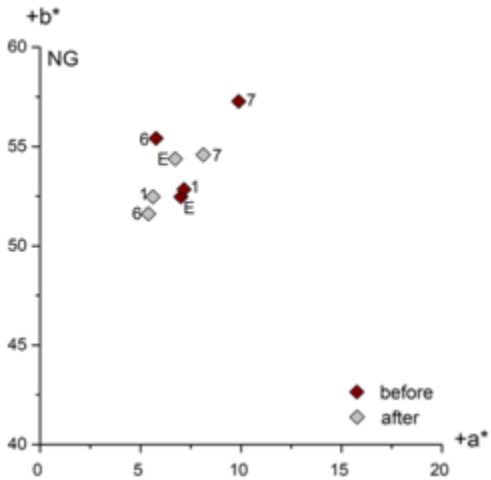

Fig.38 – a*-b* parameters for NG

Concerning the total color change (ΔE), LAY samples are clearly the ones that have changed the most before and after exposure to UV light. LTAY and NG samples show instead very low ΔE values, below five, which is considered the threshold for a visible color change to the human eye. Sample C should be probably considered an outlier; no explanation can be found for its different behaviour.

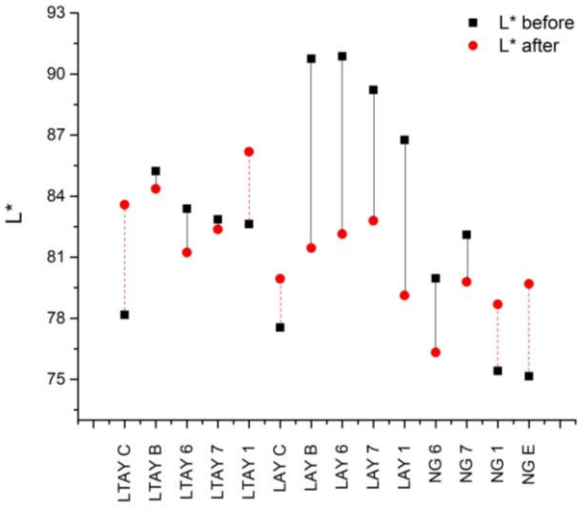

Fig.41 – L* parameter before and after aging

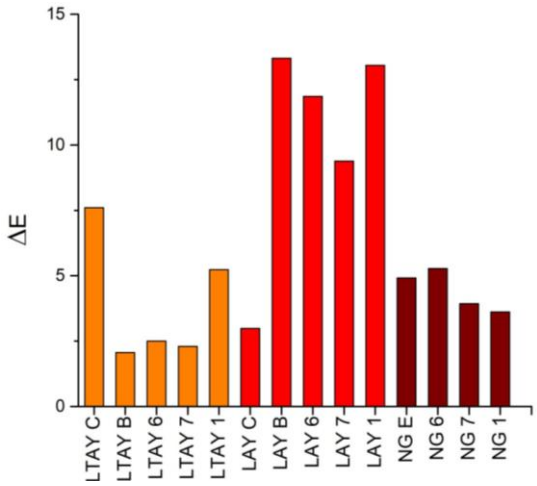

Fig.42 – Total color change ΔE

Interestingly, under UV light the colorimetric measurements results suggest that Naples yellow (LAY) is the one changing the most, while the results of the previous measurements, in particular photo-electrochemistry, showed that lead-tin-antimony yellow seems to be the pigment more prone to react towards light. This result is not necessary in contrast to the previous results showed in this study, indeed the color change might be due to an adjustement in the geometry of the bounds relative to the chromophore moieties, which does not involve any redox reaction.

Moreover, on closer inspection, in the DR-UV-Vis spectrum of LAY, an increase in the absorbance in the UV range (~350 nm) was noticed. This might indicates that LAY is more sensitive to UV light compared to LTAY, which can explain its different behaviour under UV light irradiation.

4.2.2 Chemical stability

VOCs (volatile organic compounds) are often present in museum environments. Indeed these organic pollutants are common diffusion products of wood, which is a very a popular storage material and often present in close contact with artworks. Specifically, the hydrolysis of the acetate groups in hemicelluloses causes the formation of acetic acid (CH_3COOH) and high degrees of humidity or elevate temperature can promote the process[1].

A recent study by Ghiara *et al.*[2] focused the attention on the effect of VOC-rich atmospheres, specifically employing acetic acid and formic acid, on Pb-based alloys, with antimony (Sb) and tin (Sn) as alloying elements. They experimentally showed that alloying elements, in particular under the effect of acetic acid vapors exposure, tend to influence the corrosion behavior and in particular the corrosion product formation and growth; while Sn tends to concentrate on the outer zone of the corrosion patina limiting the interaction of Pb with the environment, Sb tends to create aggregates inside the inner corrosion layer, which do not hinder the interaction between Pb and acetic acid, thus forming Pb acetates[2]. Instead, regarding the formic acid exposure, they detected lead formate on all the samples.

So, the starting idea for this study, was to check if also in the case of Pb-Sb(Sn)-based pigments the exposure to acetic and formic acid might have a degrading effect. Secondly, it was considered interesting to eventually investigate whether or not the presence Sn in the pigment composition might have an influence in the degradation process and/or in the formation of degradation products.

Samples were aged first for two weeks, subsequently new samples were aged for one month (see *par.3.2.1 Chemical aging*). Results only for mock-up samples are presented. For NG samples after exposure to formic acid studies are still undergoing.

4.2.2.1 Naples yellow (LAY)

Acetic acid exposure

After exposure to acetic acid vapors for one month rounded detachments on specific areas of the surface were observed, as shown in Fig.43. Moreover the yellow seems to have lost brightness and tends to a brownish color.

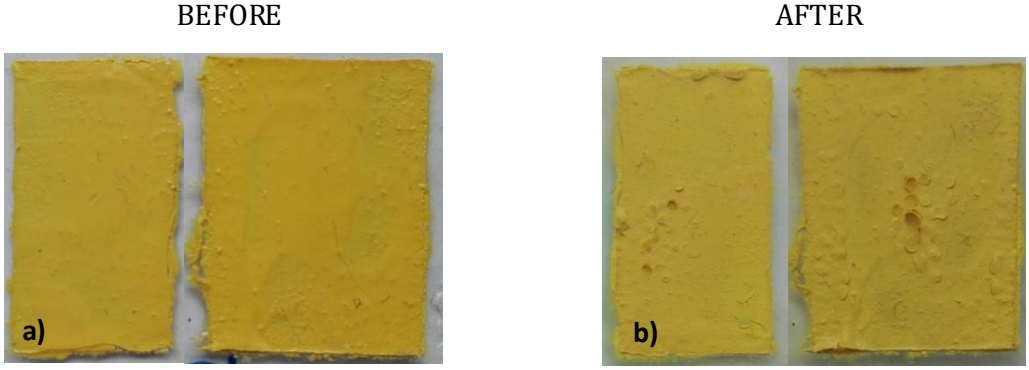

Fig.43 – Pictures of LAY samples before (a) and after (b) exposure to acetic acid vapors

Raman measurements were carried out in order to detect possible degradation products; since lead acetate was expected, previously a spectrum of lead (II) acetate basic and lead (II) acetate tryhidrate were recorded and used as references (Table 4).

Table.4 – Raman bands of reference lead acetates (red laser, 5%)

References	Main Raman bands (cm-1)*
lead (II) acetate basic	**150 vs**, 611-655 w, **930 vs**, 1338 m, 1412 m, 1533 sh, 2936 w
lead (II) acetate tryhidrate	150 sh, **202 s**, 470 w, 611 w, 662 m, **935** s, **954 vs**, **1358 s**, **1430 vs**, 2941 w

*vs=very strong, s=strong, m=medium, w=weak, sh=shoulder

No bands matching the lead acetate references or other changes in the Raman scattering features of LAY were found. It has to be considered that, because of the fluorescence of LAY sample (see par. *4.1.2*) all the peaks after 900-1000 cm^{-1} are not visible. XRD measurements were performed as well, but also in this case, no changes in the diffractogram before and after exposure to acetic acid vapors were visible. Lead acetate has a very low diffraction signal and considering also that the layer might be very thin, the identification of this compound with XRD it is challenging.

Formic acid exposure

After exposure to formic acid a clear difference in the Raman spectrum of LAY could be observed. Indeed, as shown in Fig.44 after the aging the bands relative to the pigment are not visible anymore and a high background arise. The only band still discernible is the one at ~510 cm^{-1} , which has anyway a very low intensity compared to the "not degraded" pigment.

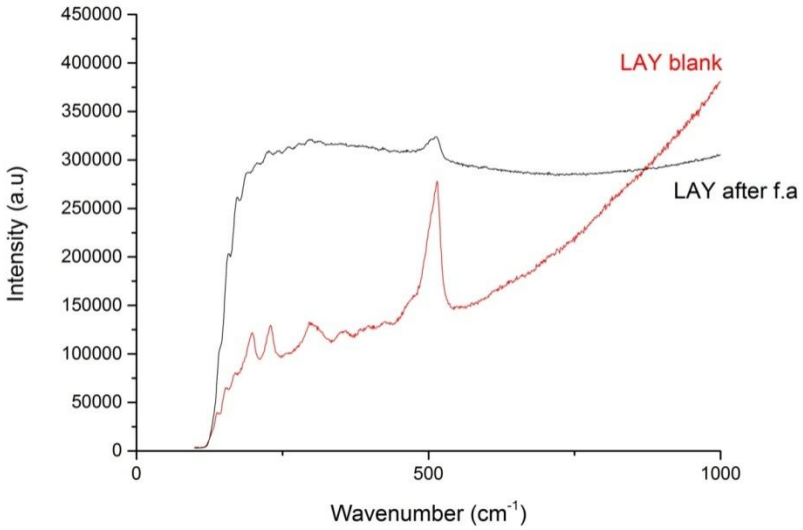

Fig.44 – Raman spectra of LAY before and after exposure to formic acid vapors (red laser, 5%)

No traces of lead formate[2], that was the expected degradation product, could be found. To better understand what was occurring on the surface of this sample, thin cross-sections were prepared and analyzed by means of Raman spectroscopy and SEM-EDX. Raman measurements, shown in Fig.46, on the cross-section were carried out starting from the surface to the bottom of the sample (Fig.45) in order to check if any difference could be found between the inner part (not exposed) and the surface (exposed).

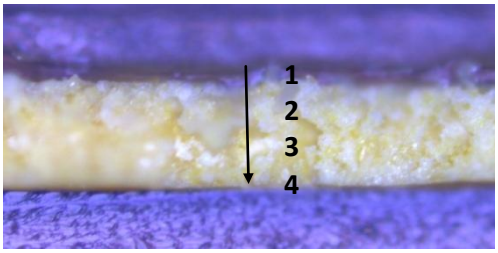

Fig.45 – Cross-section with indication of the order of the measurements

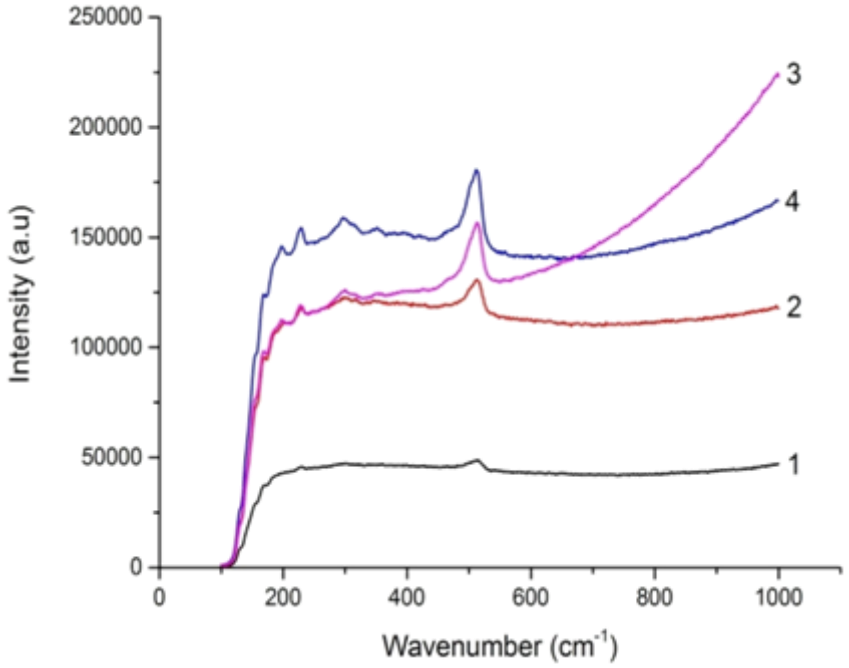

Fig.46 – Raman spectra of LAY cross-section recorded from the surface (1) to the bottom (4) (red laser, 5%)

It is clear how, proceeding from the top to the inner part, the bands relative to the pigment become more visible indicating that something it occurring on the surface and a layer of unknown composition is formed after the exposure to the formic acid vapors.

Indeed, in the SEM image (Fig.47 - a) it seems that al layer is present on the sample surface, visible also in the elemental mapping images (Fig.47 –b,c). The latter observation indicates that the layer formed has a different composition compared to the rest of the sample but EDX point measurements will be needed in order to clarify its composition.

Since in the Raman spectra of the surface layer no peaks could be recognized and the pattern of the spectrum is similar to the one of pure linseed oil in the range 100-1000 cm^{-1}, it is hypothesized that a leaching of the binding medium from the sample to the surface might have occurred. Further analysis need to be carried out to better understand the nature of the surface layer.

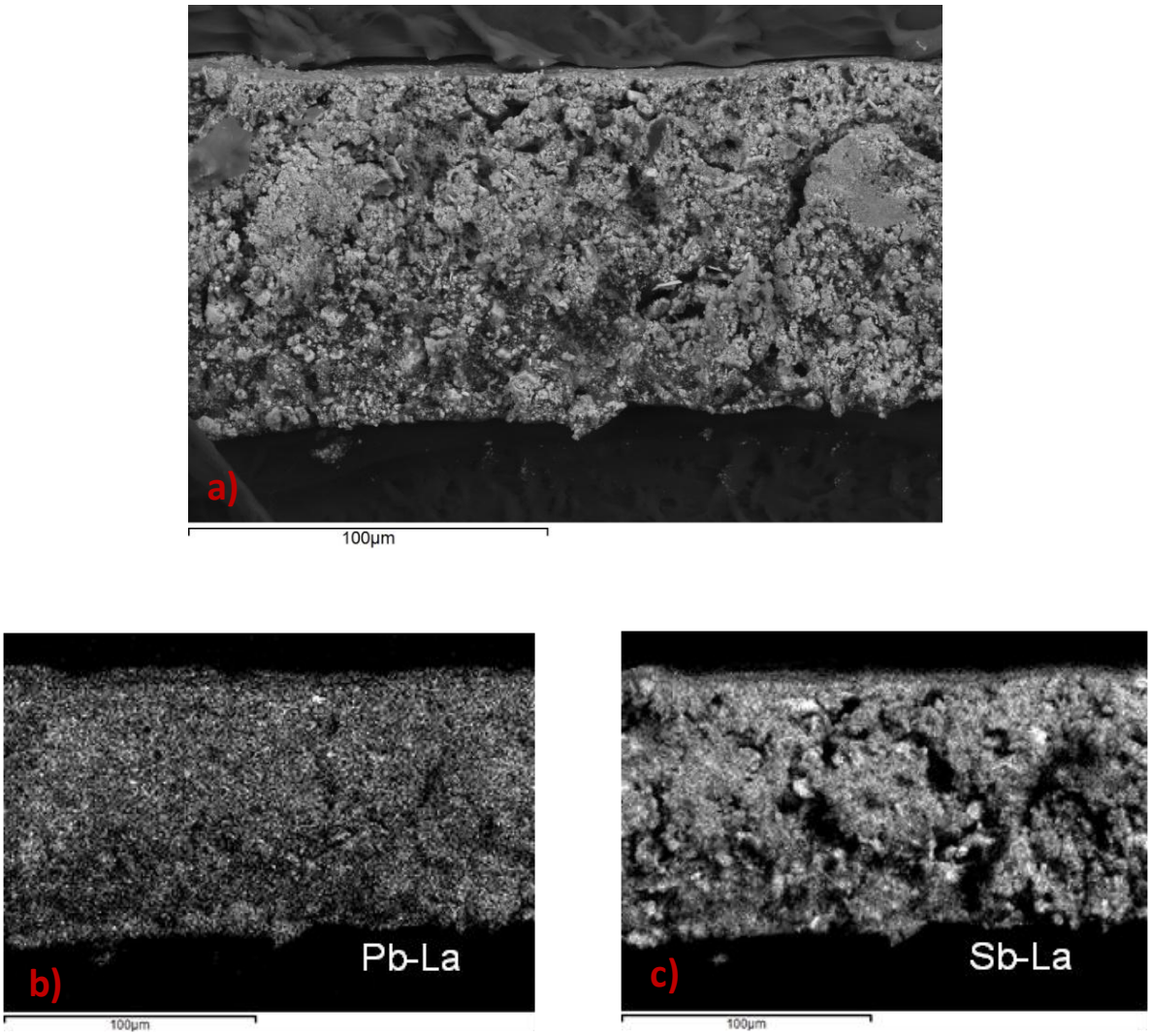

Fig.47 – SEM image of LAY cross-section (a) and elemental mapping (b,c). Livetime (s) : 1838.28, magnification : 2000X

4.2.2.2 Lead-tin-antimony yellow (LTAY)

Acetic acid exposure

After exposure to acetic acid vapors for one month a wrinkled "wet" surface was observed, as shown in Fig.48.

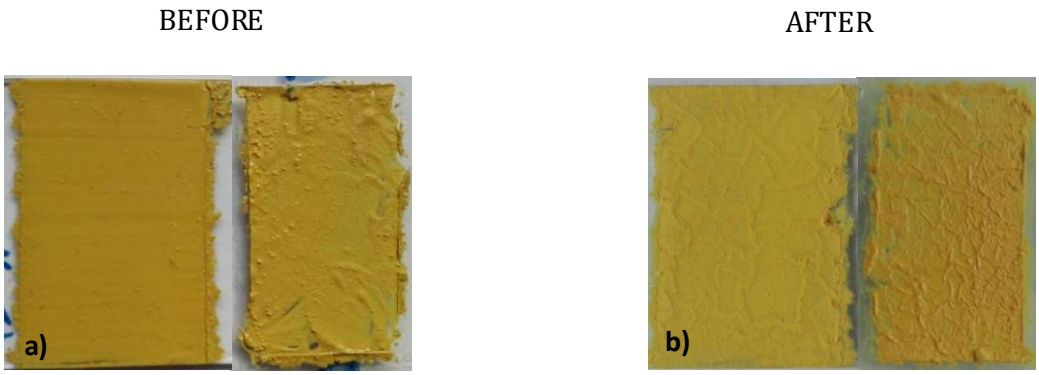

Fig.48 – Pictures of LTAY samples before (a) and after (b) exposure to acetic acid vapors

XRD measurements were carried out on the samples. As shown in Fig.49, lead tin oxide hydrate $Pb_2Sn_2H_2O_7$ was detected on one of the samples. This is probably a degradation product due to the effect of acetic acid vapors. The formation mechanism is still not clear but it was hypothesized that this compound could be an intermediate towards further degradation products such as lead acetate trihydrate ($Pb(CH_3COO)_2$ $3H_2O$) or tin (II) acetate ($Sn(CH_3COO)_2$).

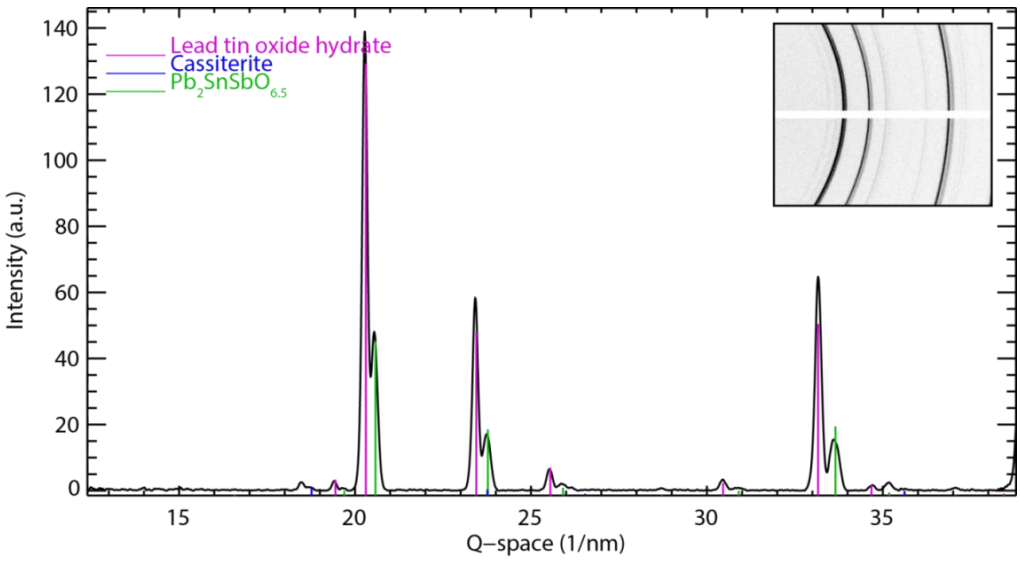

Fig.49 – Diffractogram of LTAY mock-up sample after exposure to acetic acid. Lead tin oxide hydrate is detected.

At a closer look with the Raman microscope it was noticed that on the surface of the paint some opalescent white spots were present (Fig.51 – b,c). Therefore the Raman laser was pointed at this specific spots and Raman measurement were carried out. In Fig.51 – a, the spectrum of the "not degraded" surface of lead-tin-antimony yellow is compared to the spectrum acquired on the white spot. A slight lowering of the intensity of the Raman band can be observed but no additional bands indicating the formation of a new product are visible. Considering that the layer seems to be very thin, it is possible that the laser penetrated it and the Raman scattering recorded comes from the substratum.

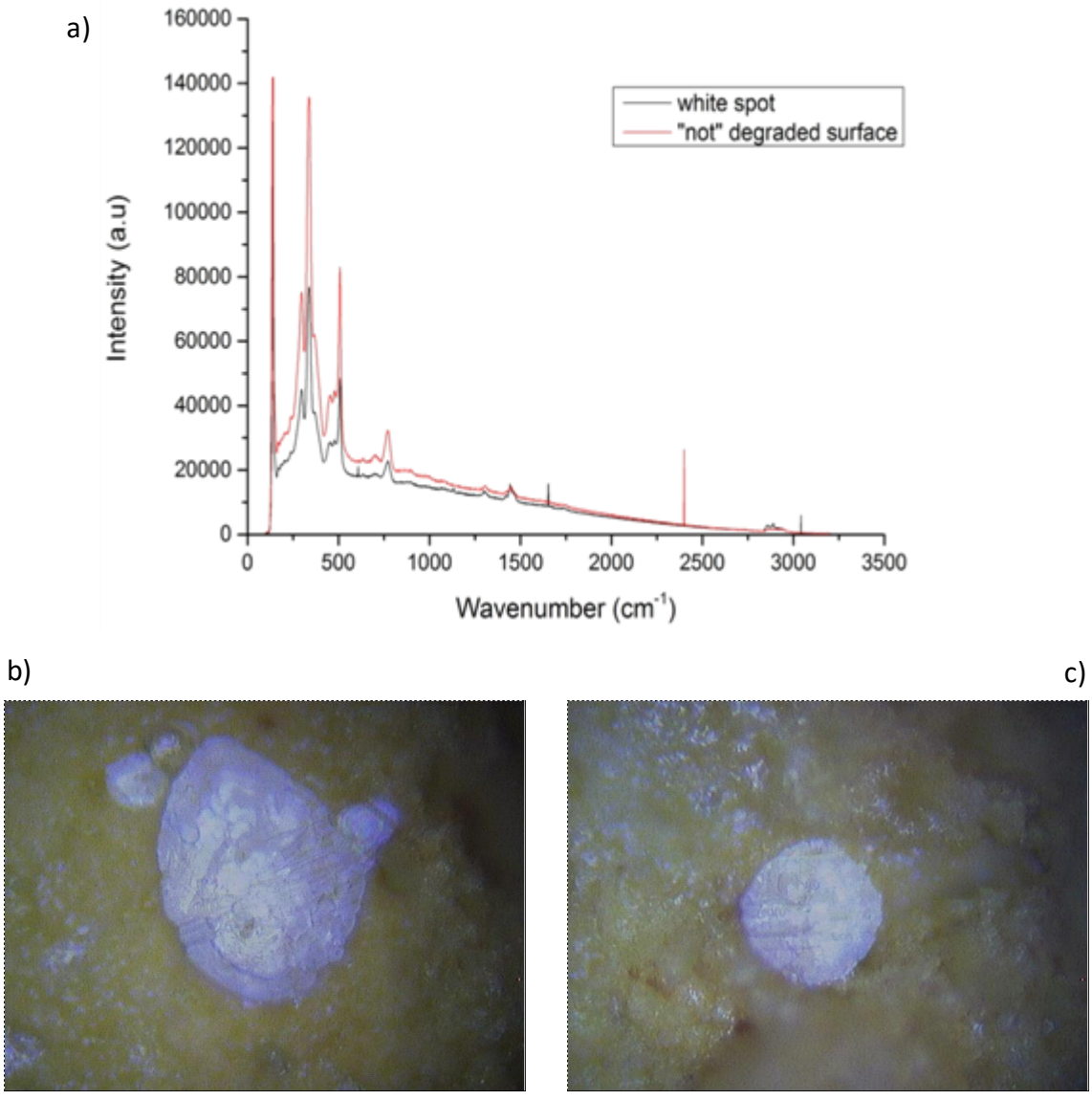

Fig.51 – Raman spectra acquired on the "not degraded" surface and on the white spot(a). Raman microscope (50x) images of the white spots present on the surface (b,c)

Concerning the exposure of LTAY samples to formic acid vapors no relevant results were observed.

4.2.2.3 Genuine Naples Yellow dark (NG)

Acetic acid exposure

After exposure to acetic acid vapors, NG samples showed a whitish patina and some white "crystals" appeared on the surface (Fig.52).

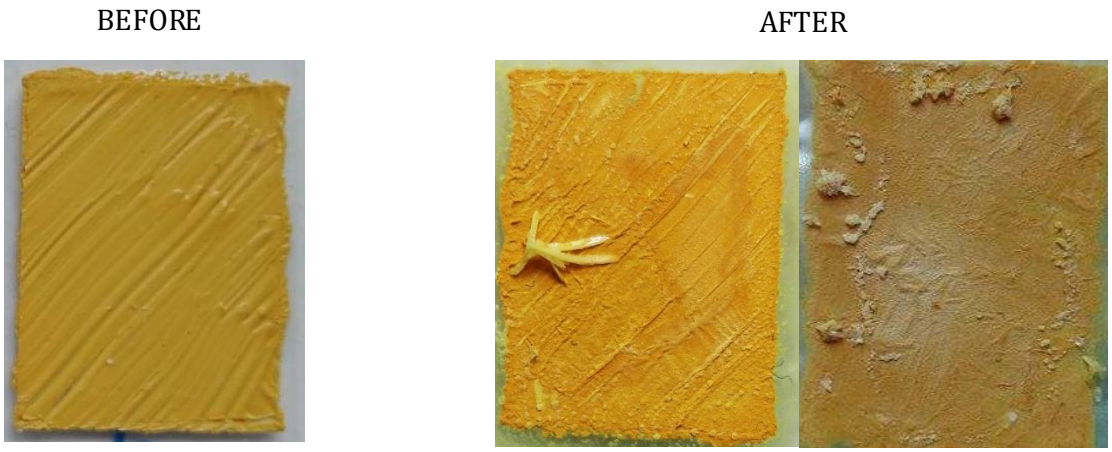

Fig.52 – Pictures of LTAY samples before (a) and after (b) exposure to acetic acid vapors

Raman measurements were performed on the crystals, on the patina and on the "not degraded" surface. As shown in Fig. 53, the bands relative to the pigment (100-1000 cm^{-1}) have a much lower intensity in the spectrum acquired on the patina (pink line), while they are not visible anymore on the spectrum recorded on the crystal (red line). Simultaneously a raise in the bands relative to the binding medium (1000-3200cm^{-1}) is observed. These results indicate that an organic compound is formed. As reported in Chapter 1 (*1.3.1 Pb-based pigment degradation*) is known from literature that lead-based pigments, including Naples yellow, when mixed with linseed oil can form lead soaps.

The network system of the polymerized oil is vulnerable to environmental attack especially by acidification that is assumed to disrupt the ionomeric structure of the binding medium[27]. As a result monocarboxylic fatty acids can be mobilized and reorganized in form in form of liquid crystalline metal soap masses within the paint

layers. When they expand beyond the paint layer they may erupt at the surface and mineralize[27]. This might be an explanation for what occurred in the samples examined in this study. Further analysis with more suitable techniques, such as FTIR or GC-MS, should be performed in order to have a proper identification of these compounds.

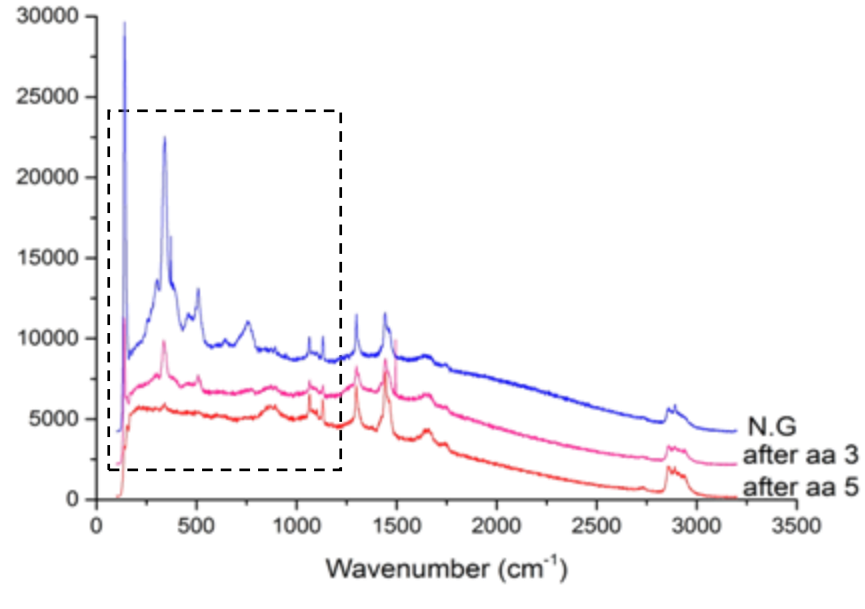

Fig.53 – Raman spectra acquired on the "not degraded" surface (blue line), on the white patina (pink line) and on the crystal (red line) of NG samples after exposure to acetic acid.

While performing Raman measurements, it was noticed that also on the NG samples opalescent, white spots, very similar to the ones observed for LTAY, occurred (Fig.54). Also in this case, Raman spectra on the white spots do not present any main difference compared to the spectra acquired on the surface. The nature of this compounds need to be clarify.

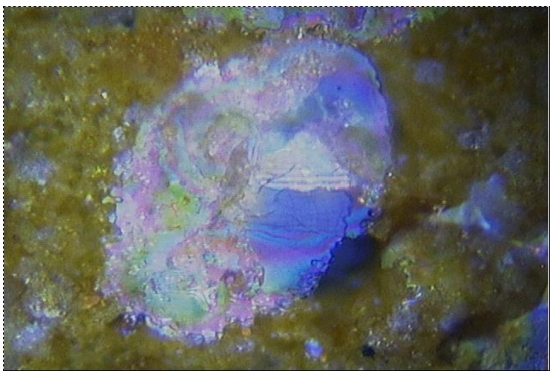

Fig.54 - Raman microscope image (50x) of the white spot present on the surface

5. Conclusions

By means of XRF, μ-Raman spectroscopy and XRD a complete overview of the chemical composition and crystalline structure of the pigments analyzed in this study was possible. Naples yellow pigment (LAY) is confirmed to have a cubic pyrochlore structure; though its composition results to be not homogeneous. Indeed, Raman and XRD measurements suggested the presence of multiple phases of $Pb_2Sb_2O_7$ with different ratios of lead and antimony. In addition, minor compounds, such as PbO, were also detected. Lead-tin-antimony yellow presents a typical structure for modified pyrochlores, where a third cation, in this case tin, enters the crystalline lattice. The pigment seems to be more homogeneous compared to Naples yellow and the only by-product detected was cassiterite (SnO_2). Concerning the commercial paint *Genuine Naples Yellow dark* (NG), unlike what declared by the manufacturer, the results of the analysis pointed out that this pigment has a composition and crystalline structure definitely more similar to lead-tin antimony yellow than pure lead antimonate. Moreover, as observed for Naples yellow, also this pigment shows different phases indicating that even 20^{th} century industrially produced yellow pyroantimonates cannot be consider composed by a pure cubic pyrochlore phase.

Concerning the stability of the pigments to light, Naples yellow (LAY) and lead-tin-antimony yellow (LTAY) showed DR-UV-vis spectra with an absorption edge typical for semiconductor compounds, therefore photo-activity (and related degradation) was expected. But, by means of photo-electrochemistry (with a supra band-gap light → blue laser), while for lead-tin-antimony yellow a photocurrent, hence a response to light, was observed, for Naples yellow almost no photo-activity was recorded. The experiment carried out with the blue laser seems to lead to the same conclusions: a change is observed for lead-tin-antimony yellow (lowering of the Raman signal), whereas no changes were observed for Naples yellow. Regarding the experiment with the green laser, pigments seems to be stable under the green light, which is in good agreement with what observed previously. Indeed, the wavelength of the green laser (532 nm) is situated at the end of the absorption edge, so it is probably not enough energetic to induce electron excitation. While carrying out the

experiments with the green laser a photo-bleaching phenomenon occurred indicating that the binding medium (linseed oil) degrades under the effect of light. Though, the degradation of the binding medium leads to the lowering of the fluorescent background that allows a better recognition of the Raman bands relative to the pigment. Finally, colorimetric measurements results after aging under UV-light indicates that Naples yellow (LAY) is the one with the major color change suggesting that higher energy (UV) is necessary to "degrade" this pigment.

Concerning the chemical stability of the pigments to organic pollutants, for Naples yellow, exposed to formic acid vapors, a possible leaching of the binding medium towards the surface was observed but not degradation products involving directly the pigment were detected. Differently, after exposure to acetic acid, on one sample of lead-tin-antimony yellow, lead tin oxide hydrate ($Pb_2Sn_2H_2O_7$) was revealed, probably an intermediate to further degradation products. Moreover, with the optical microscope, white spots were observed on the surface of lead-tin antimony yellow but XRD and Raman spectroscopy were proved to be not suitable techniques for the identification of these compounds, probably due to the too thin layer of the spots. On the commercial Naples yellow, after exposure to acetic acid, white crystals on the surface of the samples appeared. The most likely hypothesis is that lead-soaps are formed, but in order to have a certain identification of the composition of the crystals further analysis, such as FTIR or GC-MS, are necessary. In addition, white spots similar to the ones observed for lead-tin-antimony yellow, were noticed also on the commercial Naples yellow samples. It can be observed that the pigments containing also tin (LTAY and NG) seems to show similarities in the degradation products (white spots).

In conclusion the results obtained in this study suggest that Naples yellow is a quite stable pigment both under light illumination and exposure to chemical agents, while lead-tin-antimony yellow, is more prone to react under light-induced and chemical-induced degradation. It appears to be more difficult to have a clear picture of the situation regarding the stability of the commercial paint.

Some interesting insights about the stability and degradation of these pigments were given during this thesis work. It seems worth it to carry on with further studies and some challenging questions are open; in particular about the photo-activity of

lead-tin-antimony yellow and its reaction mechanism (oxidation), as well as the role of tin in the degradation processes, which seems to be a relevant factor in the stability of the pigments studied.

Bibliography

1. Dik, J., Hermens, E., Peschar, R. & Schenk, H. Early production recipes for lead antimonate yellow in Italian art. *Archaeometry* **47,** 593–607 (2005).
2. Eastaugh, N., Walsh, V., Chaplin, T. & Ruth, S. Pigment Compendium: A Dictionary and Optical Microscopy of Historical Pigments. in 226–227 (Elsevier, 2008).
3. Wainwright, I. N. M. R., Taylor, J. M., and Harley, R. D. Lead antimonate yellow. in *Artists' pigments: a handbook of their history and characteristics* (ed. Feller, R. L.) **vol.1,** 219–254 (National Gallery of Art,Washington DC, 1986).
4. Chiarantini, L. *et al.* Early Renaissance production recipes for Naples Yellow pigment: A mineralogical and lead isotope study of Italian Majolica from Montelupo (Florence). *Archaeometry* **57,** 879–896 (2015).
5. Dik, J., Peschar, R., and Schenk, H. The introduction of lead antimonate yellow in the 18th century. *Zeitschrift für Kunsttechnologie und Konserv.* **20,** 138–46 (2006).
6. Kirmizi, B., Göktürk, E. H. & Colomban, P. Colouring Agents in the Pottery Glazes of Western Anatolia: New Evidence for the Use of Naples Yellow Pigment Variations During The Late Byzantine Period. *Archaeometry* **57,** 476–496 (2015).
7. Agresti, G. I gialli di piombo, stagno, antimonio: colore e materia dell'opera d'arte. (PhD Thesis University of Tuscia, Viterbo (Italy), 2014).
8. Roy, A. & Berrie, B. H. A new lead-based yellow in the seventeenth century. *Stud. Conserv.* **43:sup1,** 160–165 (1998).
9. Sandalinas, C. & Ruiz-moreno, S. Lead-Tin-Antimony Yellow. Historical manufacture, molecular characterization and identification in seventeenth-century Italian paintings. *Stud. Conserv.* **49,** 41–52 (2004).
10. Hradil, D. *et al.* Microanalytical identification of Pb-Sb-Sn yellow pigment in historical European paintings and its differentiation from lead tin and Naples

yellows. *J. Cult. Herit.* **8,** 377–386 (2007).

11. Rosi, F. *et al.* Raman scattering features of lead pyroantimonate compounds. Part I: XRD and Raman characterization of Pb2Sb2O7 doped with tin and zinc. *J. Raman Spectrosc.* **40,** 107–111 (2009).

12. Radhakrishnan, A. N., Prabhakar Rao, P., Sibi, K. S., Deepa, M. & Koshy, P. Order-disorder phase transformations in quaternary pyrochlore oxide system: Investigated by X-ray diffraction, transmission electron microscopy and Raman spectroscopic techniques. *J. Solid State Chem.* **182,** 2312–2318 (2009).

13. Stránská, L., Šulcová, P. & Vlček, M. Synthesis and properties of inorganic pigments based on pyrochlore compounds with different lanthanides. *J. Therm. Anal. Calorim.* **113,** 127–135 (2013).

14. Mizoguchi, H., Eng, H. W. & Woodward, P. M. Probing the Electronic Structures of Ternary Perovskite and Pyrochlore Oxides Containing Sn4+ or Sb5+. *Inorg. Chem.* **43,** 1667–1680 (2004).

15. Subramanian, M. A., Aravamudan, G. & Subba Rao, G. V. Oxide pyrochlores - A review. *Prog. Solid State Chem.* **15,** 55–143 (1983).

16. Cartechini, L. *et al.* Modified Naples yellow in Renaissance majolica: study of Pb–Sb–Zn and Pb–Sb–Fe ternary pyroantimonates by X-ray absorption spectroscopy. *J. Anal. At. Spectrom.* **26,** 2500 (2011).

17. Anaf, W. The influence of particulate matter on cultural heritage. Chemical characterisation of the interaction between the atmospheric enviroment and pigments. (University of Antwerp, 2014).

18. Monico, L. *et al.* Degradation process of lead chromate in paintings by vincent van gogh studied by means of spectromicroscopic methods. 4. Artificial aging of model samples of Co-precipitates of lead chromate and lead sulfate. *Anal. Chem.* **85,** 860–867 (2013).

19. Anaf, W., Schalm, O., Janssens, K. & De Wael, K. Understanding the (in)stability of semiconductor pigments by a thermodynamic approach. *Dye. Pigment.* **113,** 409–415 (2015).

20. Anaf, W. *et al.* Electrochemical photodegradation study of semiconductor

pigments: Influence of environmental parameters. *Anal. Chem.* **86,** 9742–9748 (2014).

21. Rahemi, V. *et al.* Unique Optoelectronic Structure and Photoreduction Properties of Sulfur-Doped Lead Chromates Explaining Their Instability in Paintings. *Anal. Chem.* **89,** 3326–3334 (2017).

22. Vermeulen, M. *et al.* The darkening of copper- or lead-based pigments explained by a structural modification of natural orpiment: a spectroscopic and electrochemical study. *J. Anal. At. Spectrom.* **32,** 1331–1341 (2017).

23. Coccato, A., Moens, L. & Vandenabeele, P. On the stability of mediaeval inorganic pigments: a literature review of the effect of climate, material selection, biological activity, analysis and conservation treatments. *Herit. Sci.* **5,** 1–25 (2017).

24. De Laet, N., Lycke, S., Van Pevenage, J., Moens, L. & Vandenabeele, P. Investigation of pigment degradation due to acetic acid vapours: Raman spectroscopic analysis. *Eur. J. Mineral.* **25,** 855–862 (2013).

25. Izzo, F. C. Metal soap efflorescence in contemporary oil paintings. 430 (2014). doi:10.1007/978-3-319-10100-2

26. Noble, P., van Loon, A. & Boon, J. J. Chemical changes in old master paintings II : darkening due to increased transparency as a result of metal soap formation. *ICOM-CC, 14th Triennial Meet. Hague Prepr.* 496–503 (2005).

27. Boon, J. J., Hoogland, F. & Keune, K. Chemical Processes in Aged Oil Paints Affecting Metal Soap Migration and Aggregation. *AIC Paint. Spec. Gr. Postprints* 18–32 (2007).

28. Higgitt, C., Spring, M. & Saunders, D. Pigment-medium Interactions in Oil Paint Films containing Red Lead or Lead-tin Yellow. *Natl. Gall. Tech. Bull.* **24,** 75–95 (2003).

29. Mazzeo, R. *Analytical Chemistry for Cultural Heritage*. (Springer International Publishing, 2017).

30. Keune, K., Hoogland, F., Boon, J. J., Peggie, D. & Higgitt, C. Evaluation of the 'added value' of SIMS: A mass spectrometric and spectroscopic study of an

unusual Naples yellow oil paint reconstruction. *Int. J. Mass Spectrom.* **284,** 22–34 (2009).

31. Tumosa, C. S. & Mecklenburg, M. F. The influence of lead ions on the drying of oils. *Stud. Conserv.* **50,** 39–47 (2005).

32. Van der Weerd, J. Microspectroscopic analysis of traditional oil paint. (University of Amsterdam, 2002).

33. Field, G. *Chromatography; or, A treatise on colours and pigments, and of their powers in painting*. (London, C. Tilt, 1835).

34. Church, A. H. *The chemistry of paints and paintings*. (1915).

35. Michael Harding | Artist quality handmade oil colours. Available at: http://www.michaelharding.co.uk/.

36. Smith, G. D. & Clark, R. J. H. Raman microscopy in archaeological science. *J. Archaeol. Sci.* **31,** 1137–1160 (2004).

37. Smith, G. D. & Clark, R. J. H. Raman microscopy in art history and conservation science. *Stud. Conserv.* **46,** 92–106 (2001).

38. López, R. & Gómez, R. Band-gap energy estimation from diffuse reflectance measurements on sol-gel and commercial TiO2: A comparative study. *J. Sol-Gel Sci. Technol.* **61,** 1–7 (2012).

39. Poldi, G. & Villa, G. C. F. *Dalla conservazione alla storia dell'arte: Riflettografia e analisi non invasive per lo studio dei dipinti*. (Edizioni della Normale, 2006).

40. Raman spectroscopy. Available at: https://www.xrite.com/.

41. XRD. Available at: https://serc.carleton.edu/research_education/geochemsheets/techniques/XRD.html.

42. Rosi, F. *et al.* Raman scattering features of lead pyroantimonate compounds: Implication for the non-invasive identification of yellow pigments on ancient ceramics. Part II. in situ characterisation of Renaissance plates by portable micro-Raman and XRF studies. *J. Raman Spectrosc.* **42,** 407–414 (2011).

43. Agresti, G., Baraldi, P., Pelosi, C. & Santamaria, U. Yellow pigments based on lead,

tin, and antimony: Ancient recipes, synthesis, characterization, and hue choice in artworks. *Color Res. Appl.* **41,** 226–231 (2016).

44. Dik, J., Tichelaar, F., Goubitz, K., Peschar, R., and Schenk, H. 19th century Naples Yellow re-examinated. *Zeitschrift für Kunsttechnologie und Konserv.* **16,** 291–306 (2002).

45. Sakellariou, K., Miliani, C., Morresi, A. & Ombelli, M. Spectroscopic investigation of yellow majolica glazes. *J. Raman Spectrosc.* **35,** 61–67 (2004).

46. Dennis, A. Photo-Bleaching and Automatic Baseline Correction for Raman Spectroscopy. (2007). Available at: http://www.perkinelmer.de/CMSResources/Images/44-74254APP_RamanPhoto-BleachingAutoCorrection.pdf.

47. Macdonald, A. M. & Wyeth, P. On the use of photobleaching to reduce fluorescence background in Raman spectroscopy to improve the reliability of pigment identification on painted textiles. *J. Raman Spectrosc.* **37,** 830–835 (2006).

48. Ghiara, G. *et al.* Micro Raman investigation on corrosion of pbbased alloy Replicas of letters from the museum Plantin-Moretus, Antwerp. *J. Raman Spectrosc.* **45,** 1093–1102 (2014).